

Dynamics of PBH clusters & predictions for GW observatories

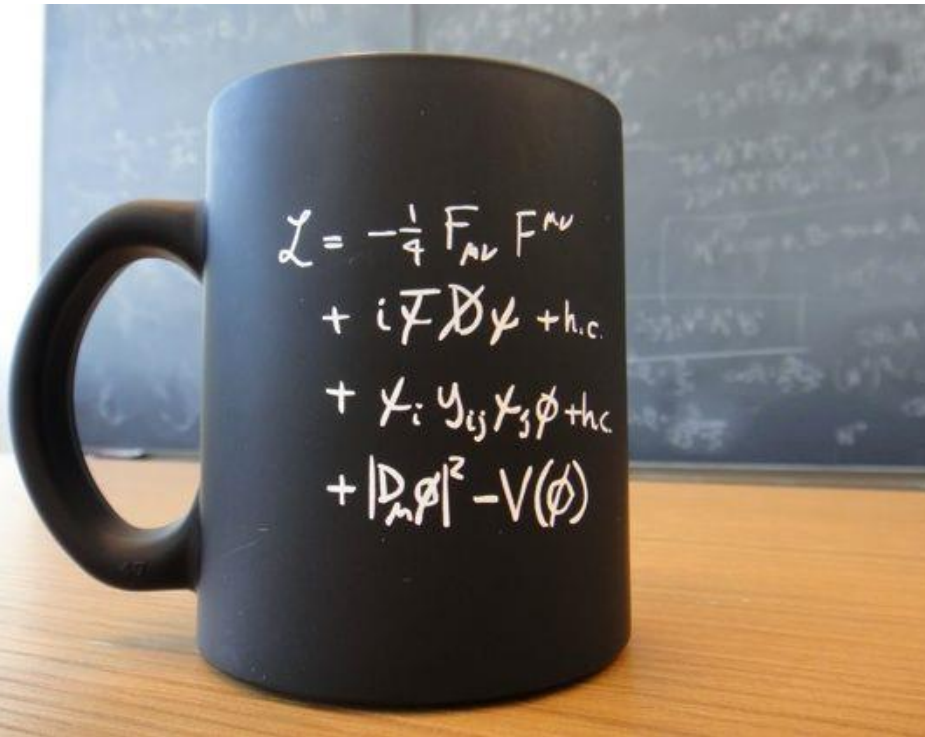
Focus Week PBH, IPMU, 13th Nov 2024

Juan García-Bellido
IFT-UAM/CSIC

Outline

- Fundamental Physics and PBH:
 - Critical Higgs Inflation
 - Quantum Diffusion and PNG tails
- PBH cluster dynamics:
 - Binary parameter distributions
 - Spin induction in dense clusters
- Observational Evidences:
 - Gravitational Waves (GWTC-3)

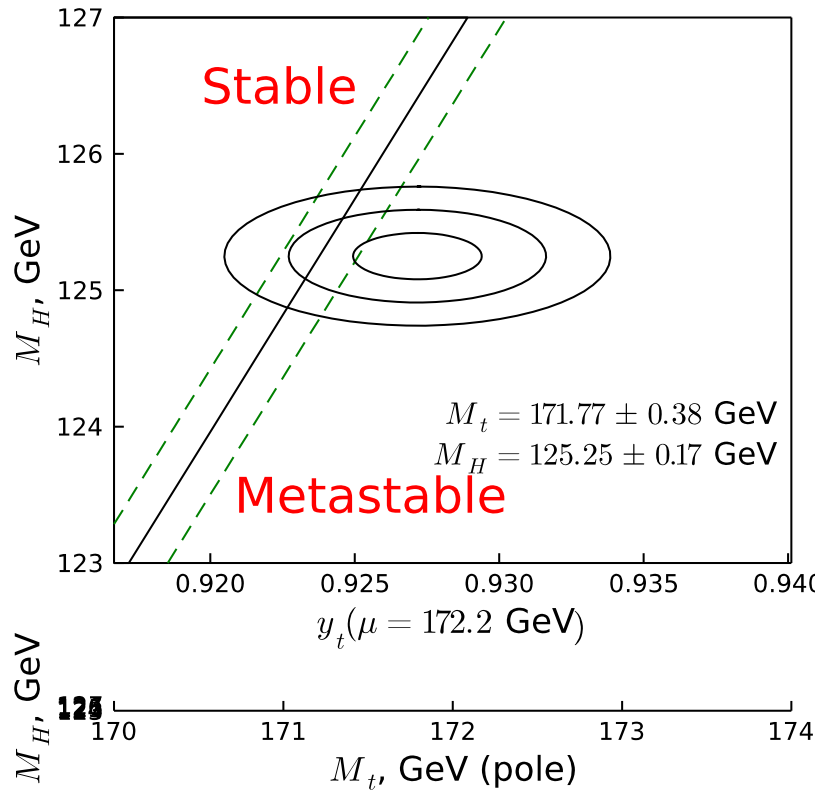
Standard Model Lagrangian



$$\begin{aligned} \mathcal{L} = & -\frac{1}{4} F_{\mu\nu} F^{\mu\nu} \\ & + i\bar{\Psi}\not{D}\Psi + \text{h.c.} \\ & + \bar{\Psi}_i y_{ij} \Psi_j \phi + \text{h.c.} \\ & + |D_\mu \phi|^2 - V(\phi) \\ & + \sum_i |\phi_i|^2 R \end{aligned}$$

$$R = 12H^2 + 6\dot{H} \rightarrow R_0 = 9.2 H_0^2 \rightarrow m_H = \sqrt{\xi R_0} = 2 \times 10^{-32} \text{ eV}$$

EW vacuum metastability

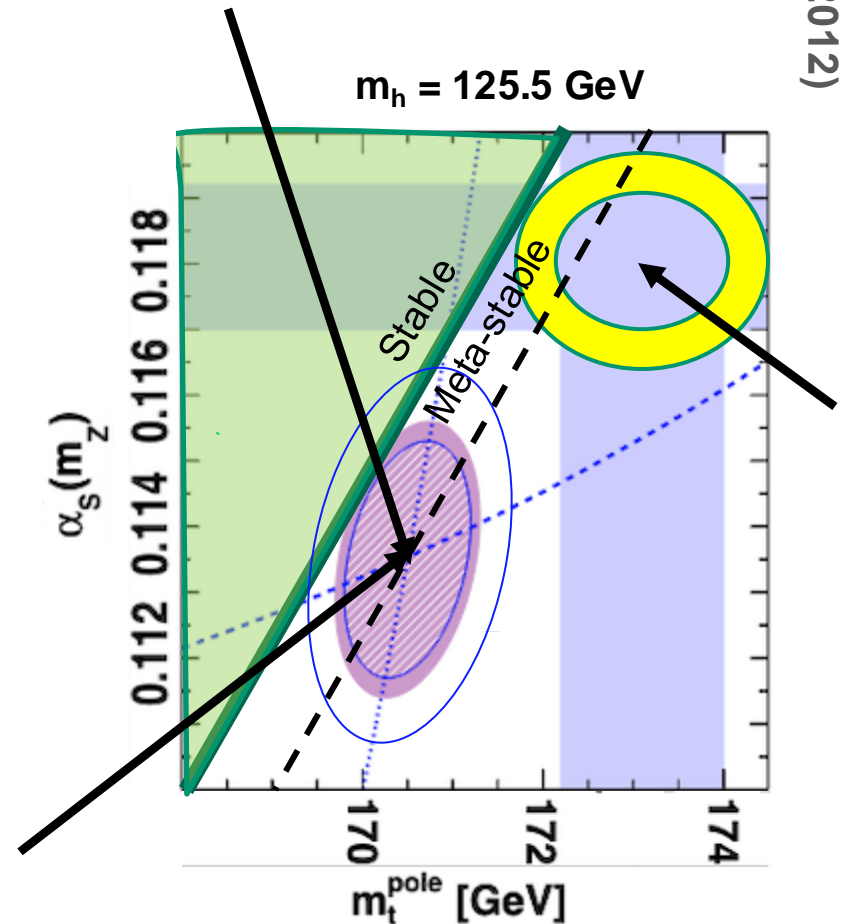


$$m_t^{\text{pole}} = 170.5 \pm 0.8 \text{ GeV}$$

$$\alpha_S(m_Z) = 0.1135^{+0.0021}_{-0.0017}$$

LHC-CMS Collab. (2020)

<https://arxiv.org/abs/1904.05237>



Buttazzo et al.
(2012)

<https://arxiv.org/pdf/1112.3022.pdf>

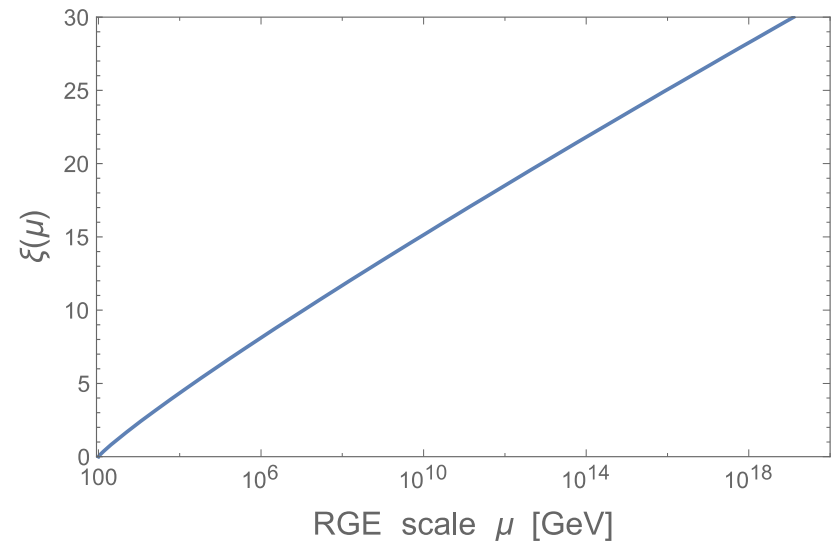
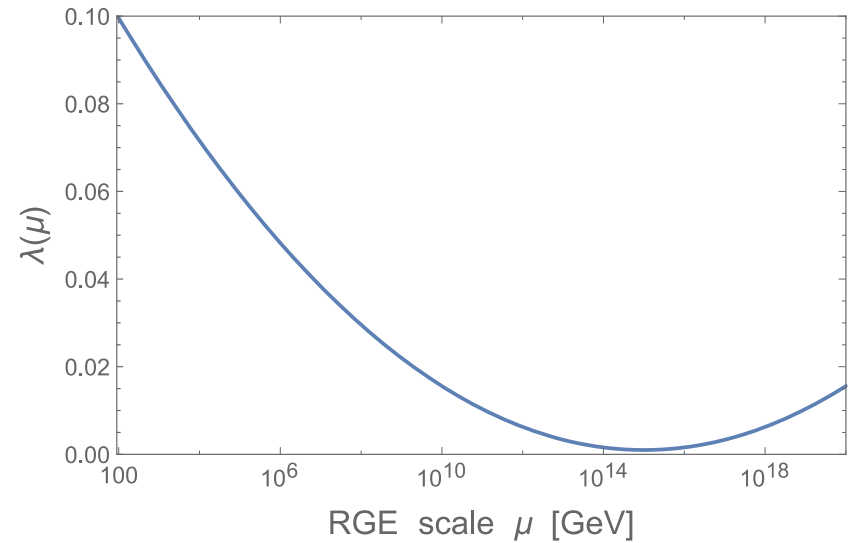
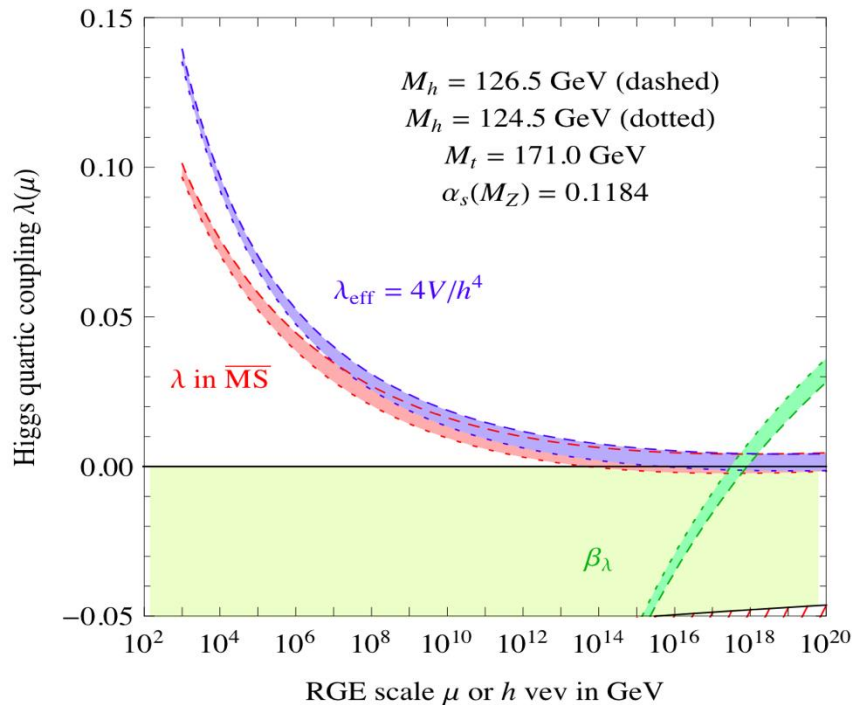
Renormalization of Higgs couplings

Ezquiaga, JGB, Ruiz [1705.04861]

$$\lambda(\phi) = \lambda_0 + b_\lambda \ln^2(\phi/\mu),$$

$$\xi(\phi) = \xi_0 + b_\xi \ln(\phi/\mu),$$

Buttazzo et al (2014)



Critical Higgs Inflation

Ezquiaga, JGB, Ruiz Morales [1705.04861]

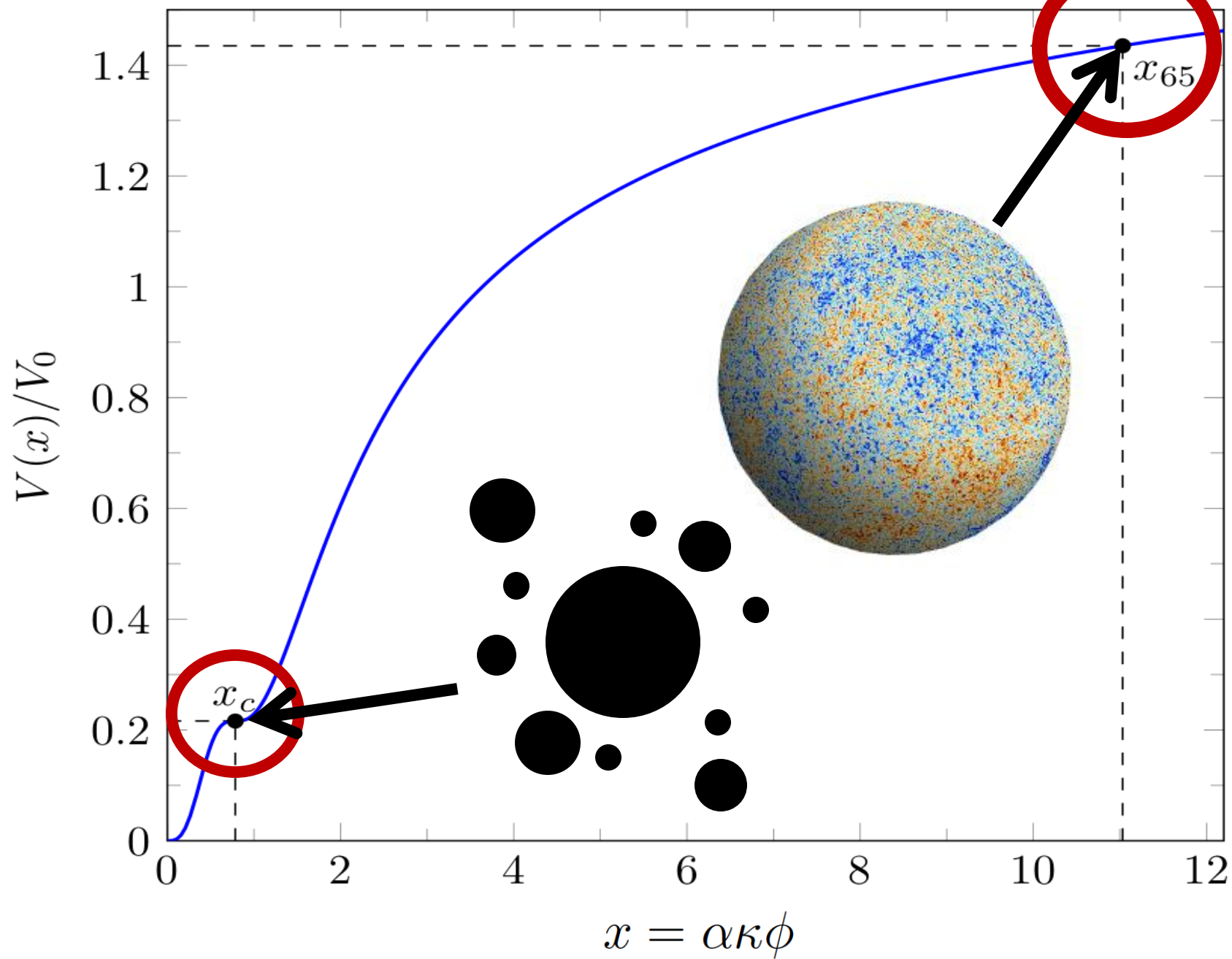
$$S = \int d^4x \sqrt{g} \left[\left(\frac{1}{2\kappa^2} + \frac{\xi(\phi)}{2} \phi^2 \right) R - \frac{1}{2} (\partial\phi)^2 - \frac{1}{4} \lambda(\phi) \phi^4 \right]$$

$$g_{\mu\nu} \rightarrow h_{\mu\nu} = (1 + \xi\phi^2) g_{\mu\nu} \quad \begin{aligned} \lambda(\phi) &= \lambda_0 + b_\lambda \ln^2(\phi/\mu) , \\ \xi(\phi) &= \xi_0 + b_\xi \ln(\phi/\mu) , \end{aligned}$$

$$\frac{d\varphi}{d\phi} = \frac{\sqrt{1 + \xi(\phi) \phi^2 + 6 \phi^2 (\xi(\phi) + \phi \xi'(\phi)/2)^2}}{1 + \xi(\phi) \phi^2}$$

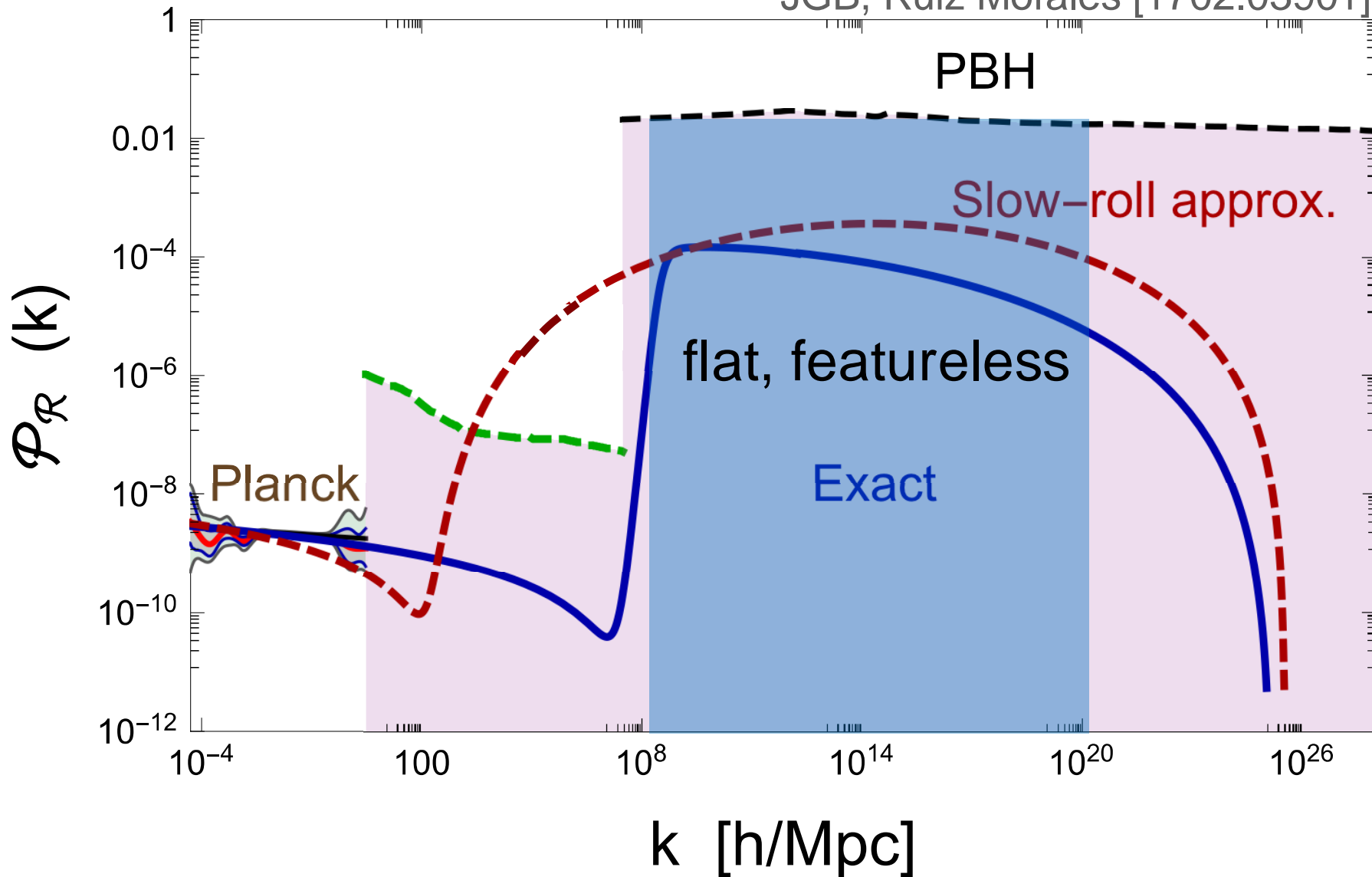
$$V(x) = \frac{V_0 (1 + a \ln^2 x) x^4}{(1 + c (1 + b \ln x) x^2)^2} \quad x = \phi/\mu$$

$$V_0 = \lambda_0 \mu^4 / 4, \quad a = b_\lambda / \lambda_0, \quad b = b_\xi / \xi_0 \quad \text{and} \quad c = \xi_0 \kappa^2 \mu^2$$

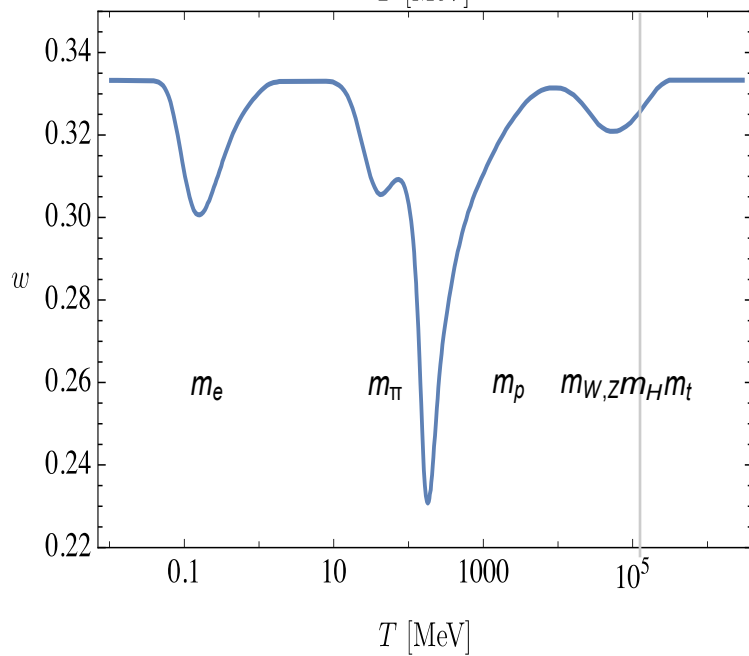
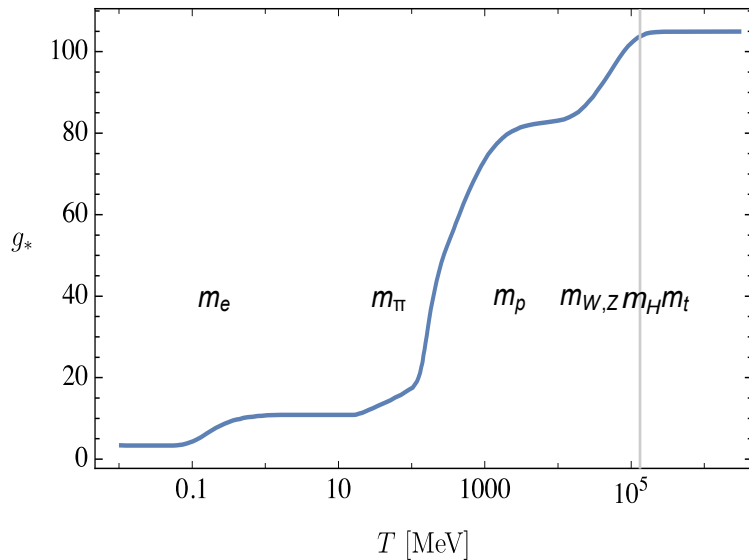


Primordial Power Spectrum

JGB, Ruiz Morales [1702.03901]

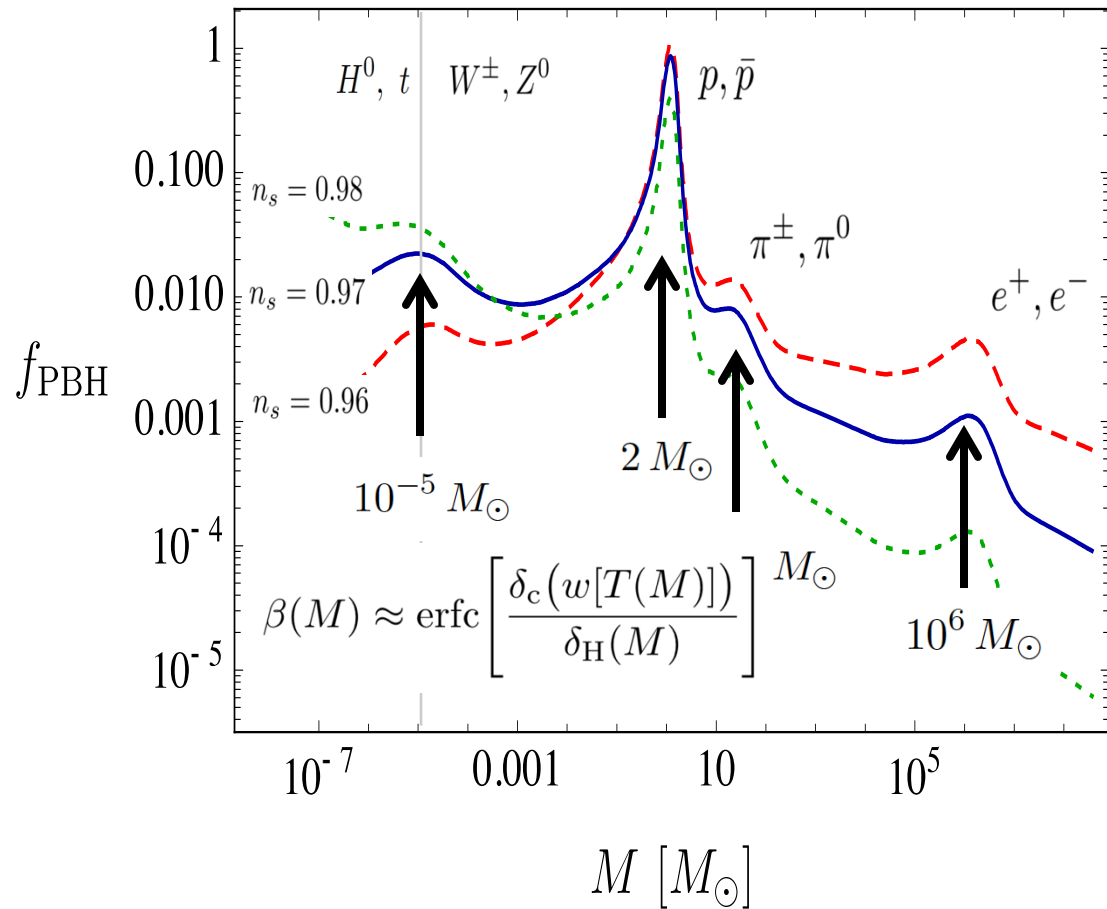


Thermal history of the universe

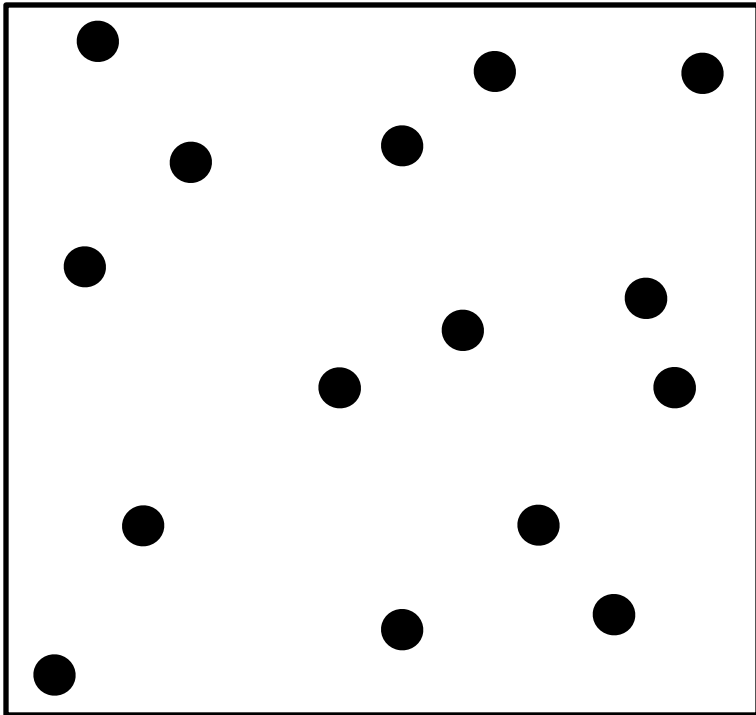


Carr, Clesse, JGB, Kühnel [1906.08217]

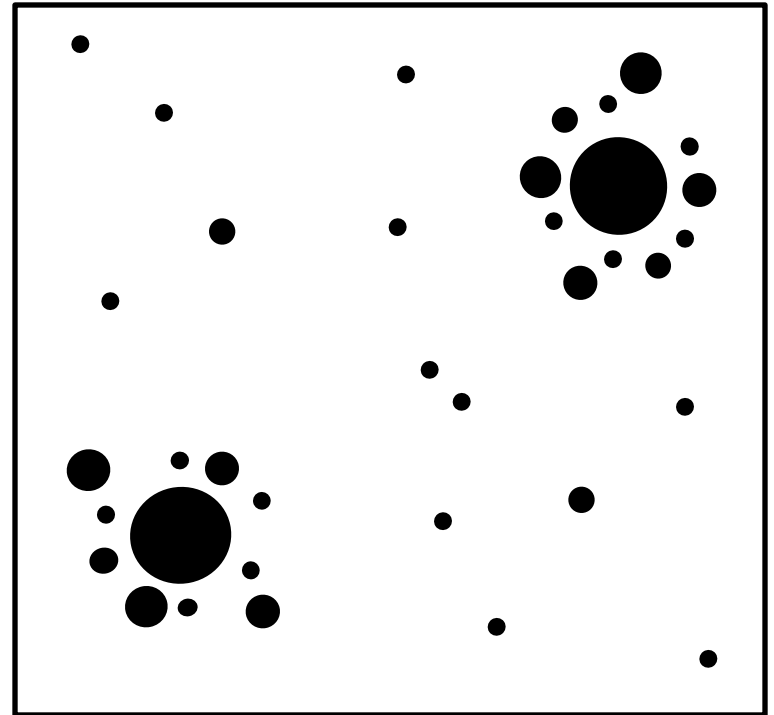
PBH mass spectrum



What about clustering of PBH?



- Monochromatic
- Uniformly distributed



- Broad range of masses
- PBH in clusters

Stochastic δN - formalism

Coarse-grained curvature perturbation

$$ds^2 = -dt^2 + a^2(t)e^{2\zeta(t, \mathbf{x})} \delta_{ij} dx^i dx^j \quad \zeta_{\text{cg}}(\mathbf{x}) = \delta N_{\text{cg}}(\mathbf{x}) = \mathcal{N}(\mathbf{x}) - \langle \mathcal{N} \rangle$$

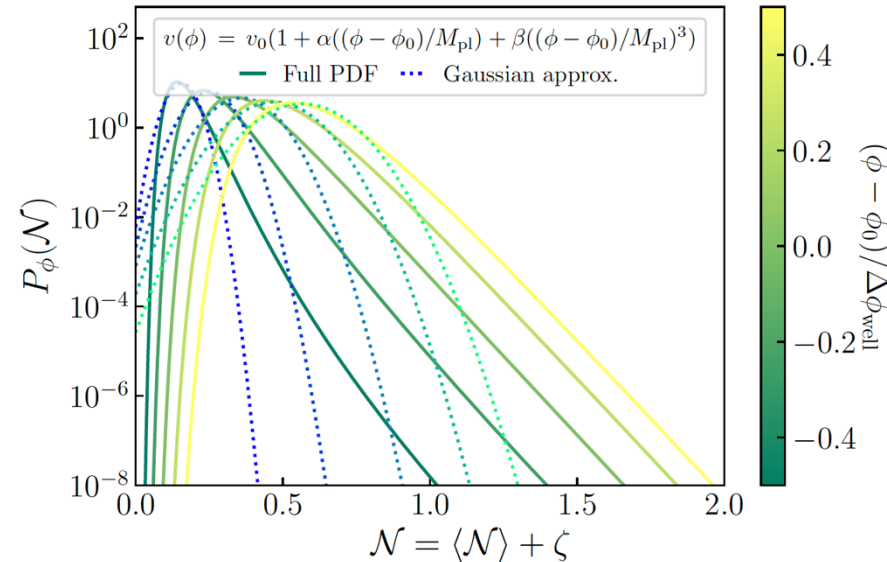
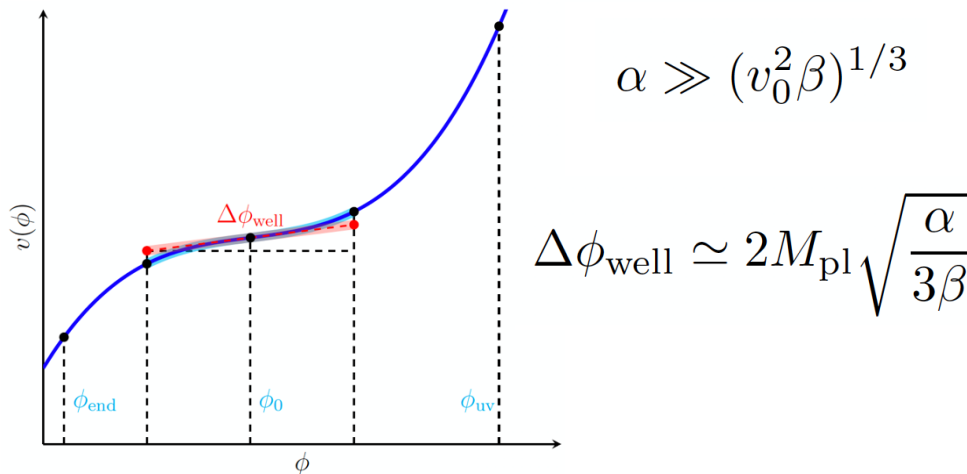
$$\frac{1}{M_{\text{pl}}^2} \frac{d}{d\mathcal{N}} P_{\Phi}(\mathcal{N}) = \left(- \sum_i \frac{v_{\phi_i}}{v} \frac{\partial}{\partial \phi_i} + v \sum_i \frac{\partial^2}{\partial \phi_i^2} \right) \cdot P_{\Phi}(\mathcal{N}) \quad \text{Fokker-Planck Diffusion Eq.}$$

Determined by the poles of the characteristic function

$$P_{\phi}(\mathcal{N}) = \frac{1}{2\pi} \int_{-\infty}^{\infty} e^{-it\mathcal{N}} \chi_{\mathcal{N}}(t, \phi) dt = \sum_n a_n(\phi) e^{-\Lambda_n \mathcal{N}}$$

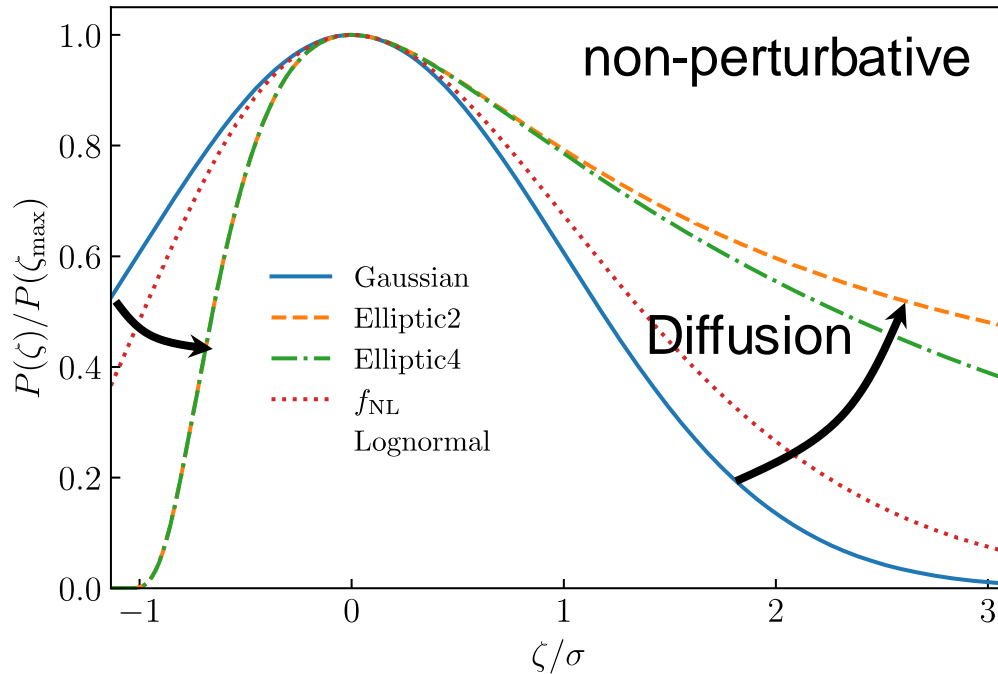
$$\chi_{\mathcal{N}}(t, \phi) = \sum_n \frac{a_n(\phi)}{\Lambda_n - it} + \text{regular func.}$$

Ezquiaga, JGB, Vennin [1912.05399]



Quantum Diffusion \ni CMB & LSS

Ezquiaga, JGB, Vennin [2207.06317]



Elliptic Functions

$$P_2(\zeta_k) = -\frac{\pi}{2\mu^2} \vartheta'_2 \left(\frac{\pi\alpha_k}{2}, e^{-\frac{\pi^2}{\mu^2} \mathcal{N}_k} \right)$$

$$P_4(\zeta_k) = \frac{\pi}{2\mu^2\alpha_k} \vartheta'_4 \left(\frac{\pi\alpha_k}{2}, e^{-\frac{\pi^2}{\mu^2} \mathcal{N}_k} \right)$$

f_{NL} – expansion (not enough)

$$\zeta(x) = \zeta_{\text{G}}(x) + \frac{3}{5} f_{\text{NL}} \left[\zeta_{\text{G}}^2(x) - \sigma_{\text{G}}^2(x) \right]$$

Lognormal distributions

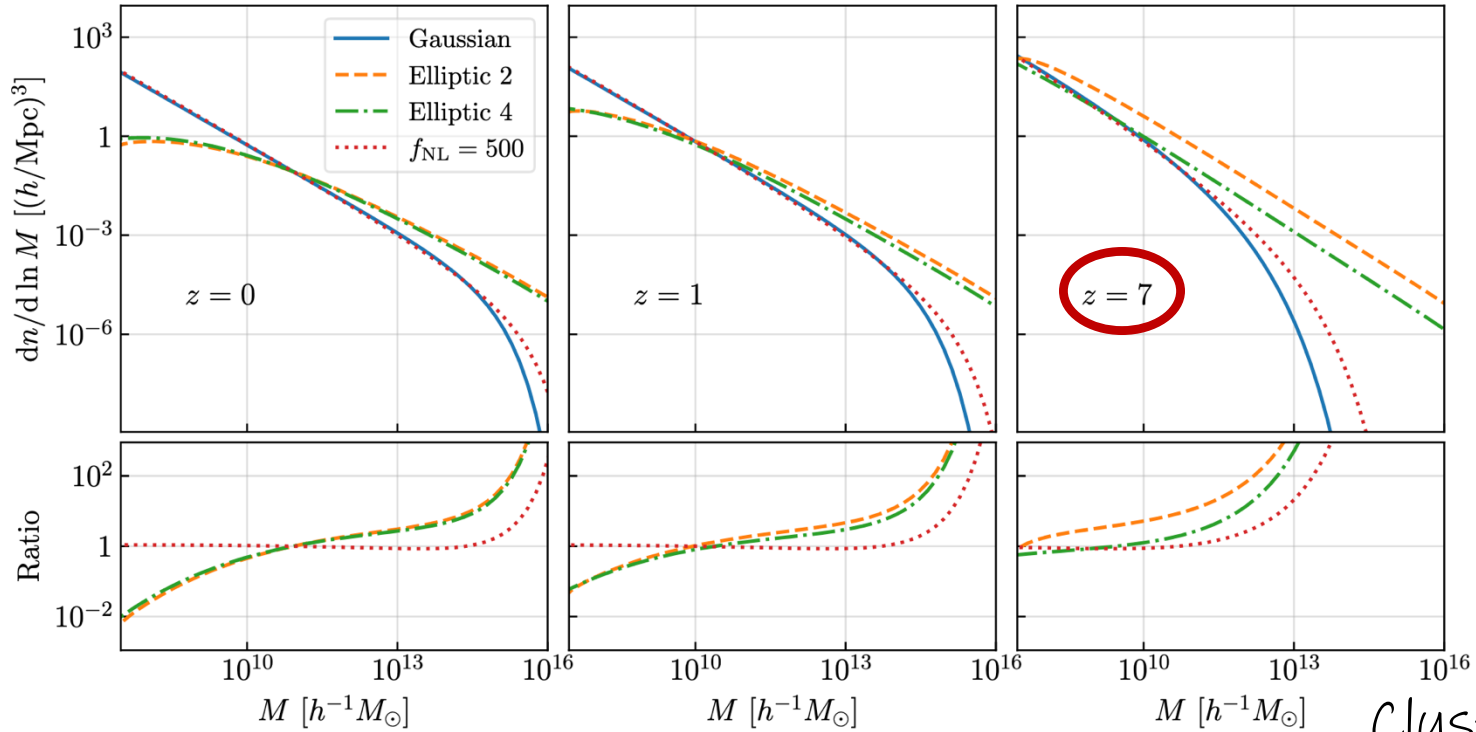
$$\text{LN}(x, \rho, \sigma) = \frac{1}{\rho\sigma\sqrt{2\pi}} \exp \left[-\frac{\ln(x/\rho)^2}{2\sigma^2} - \frac{\sigma^2}{2} \right]$$

$$\text{G}(x, \rho, \sigma_{\text{G}}) = \frac{1}{\sigma_{\text{G}}\sqrt{2\pi}} \exp \left[-\frac{(x - \rho)^2}{2\sigma_{\text{G}}^2} \right]$$

$$P_{\text{NL}}(\zeta) = \frac{1}{\sqrt{2\pi\sigma_{\text{G}}^2\Delta}} \left[e^{-\frac{25(\sqrt{\Delta}-1)^2}{72f_{\text{NL}}^2\sigma_{\text{G}}^2}} + e^{-\frac{25(\sqrt{\Delta}+1)^2}{72f_{\text{NL}}^2\sigma_{\text{G}}^2}} \right]$$

where $\Delta(\zeta) = 1 + \frac{12}{5} f_{\text{NL}}\zeta + \frac{36}{25} f_{\text{NL}}^2\sigma_{\text{G}}^2$.

Quantum Diffusion \leadsto CMB & LSS



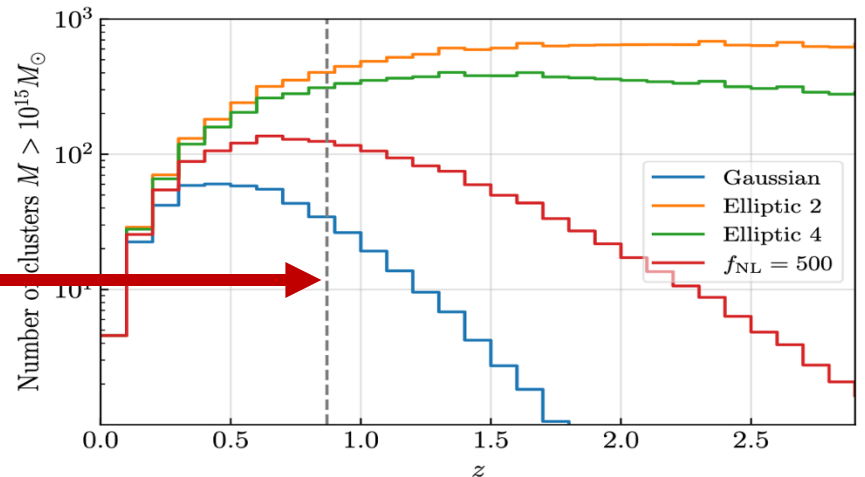
Halo
Mass
Function

Cluster Abundance

Ezquiaga, JGB, Vennin [2207.06317]

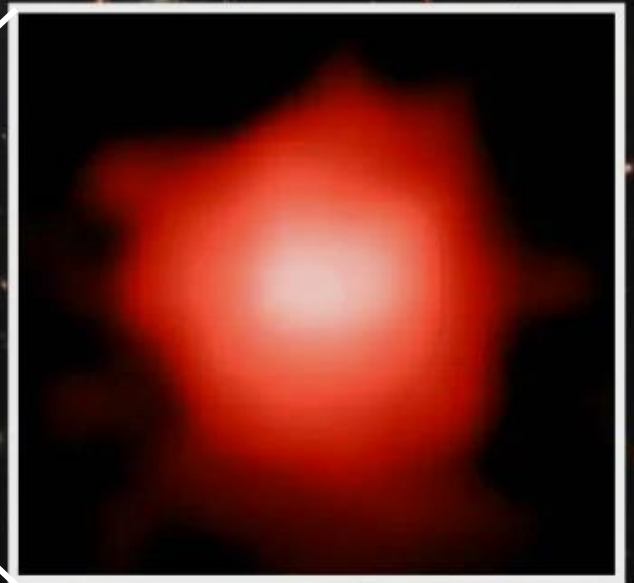
El Gordo

$M \sim 3 \cdot 10^{15} M_{\odot}$ at $z = 0.87$



PBH could explain the SMBH in the
center of galaxies seen by JWST at
 $z \sim 13-16$

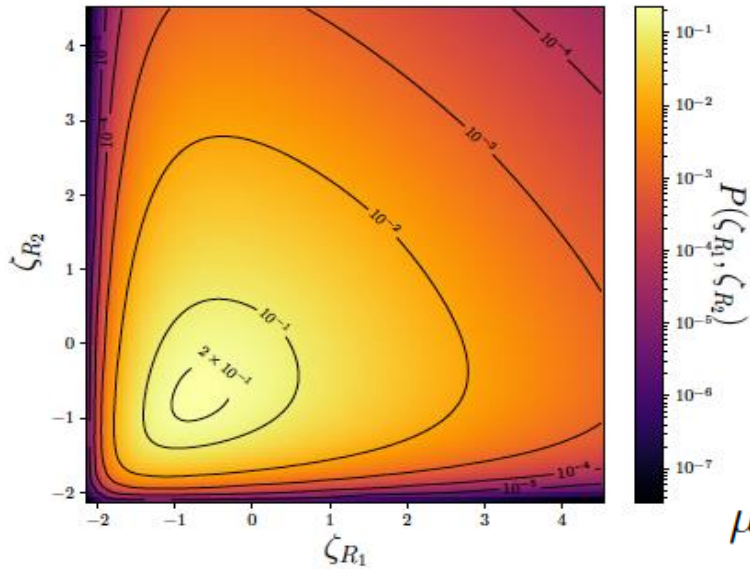
JGB, Clesse [1501.07565]
Ezquiaga, JGB, Vennin [2207.06317]



Clustering from Quantum Diffusion

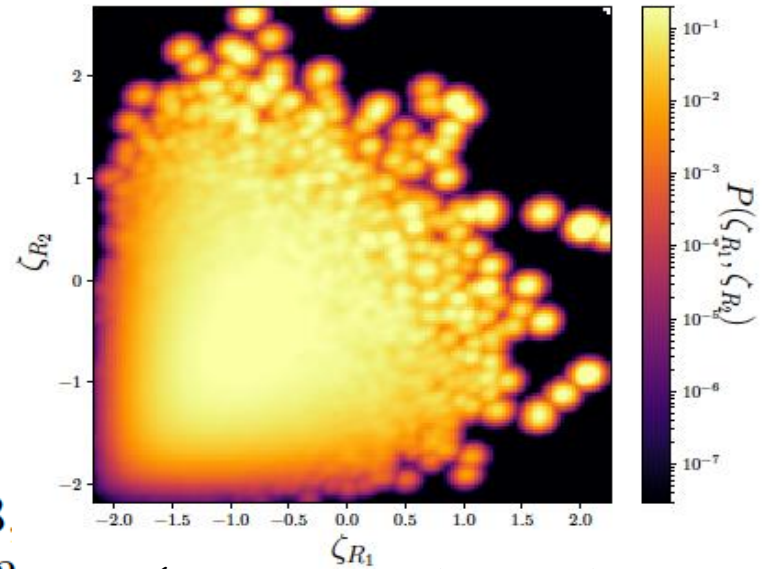
2-pt distribution function

Animali, Vennin [2402.08642]

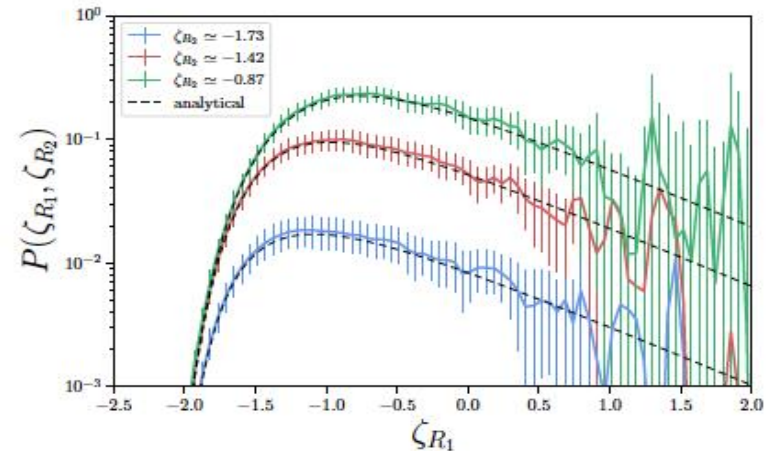
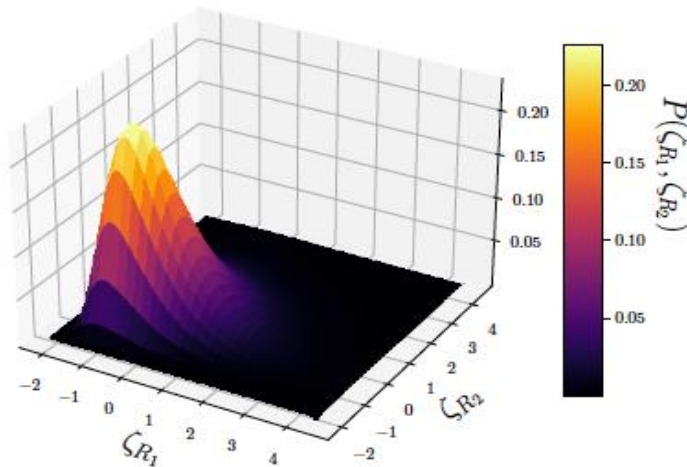


Tilted-well potential

$\mu = 13$
 $d = 0.3$

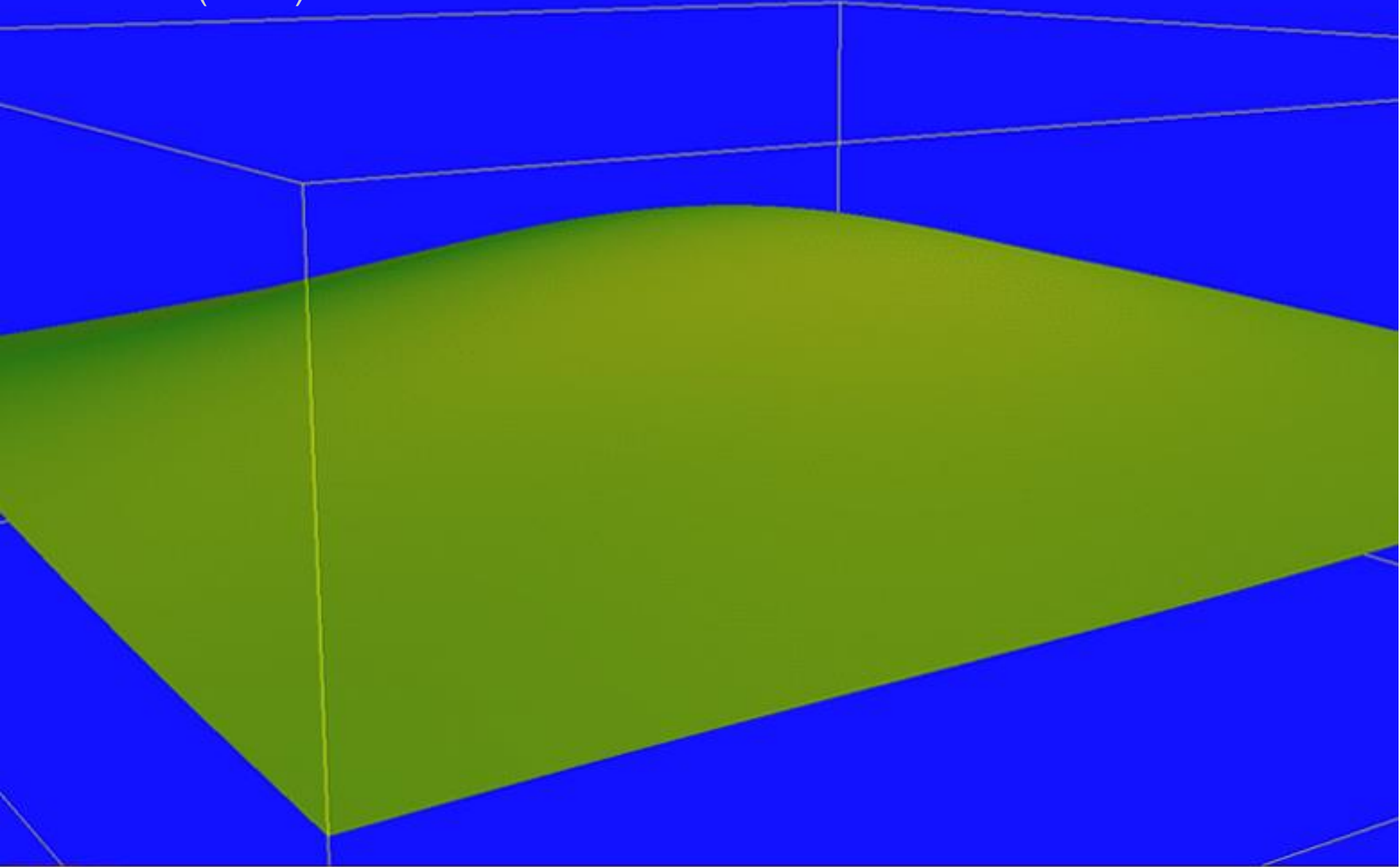


10^6 numerical simulations

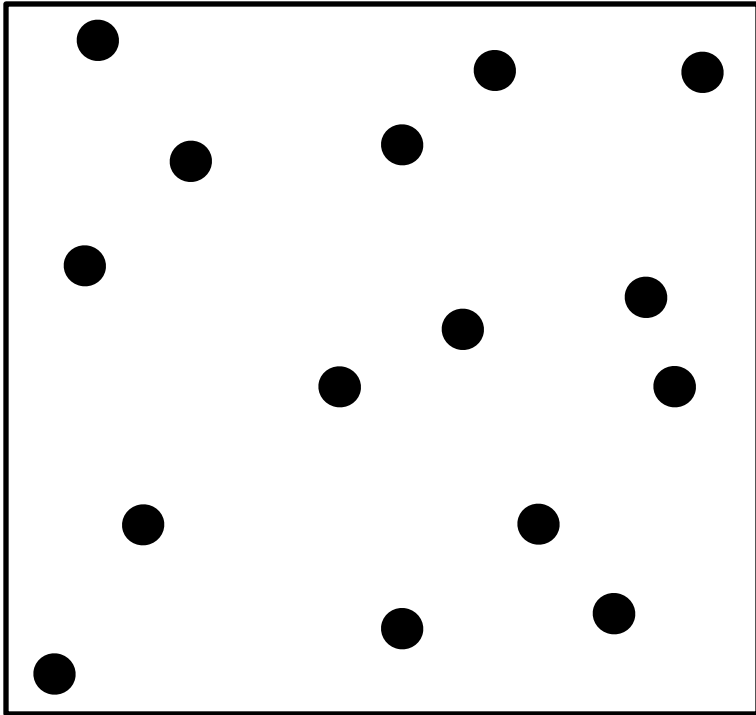


PBH and Stochastic Inflation

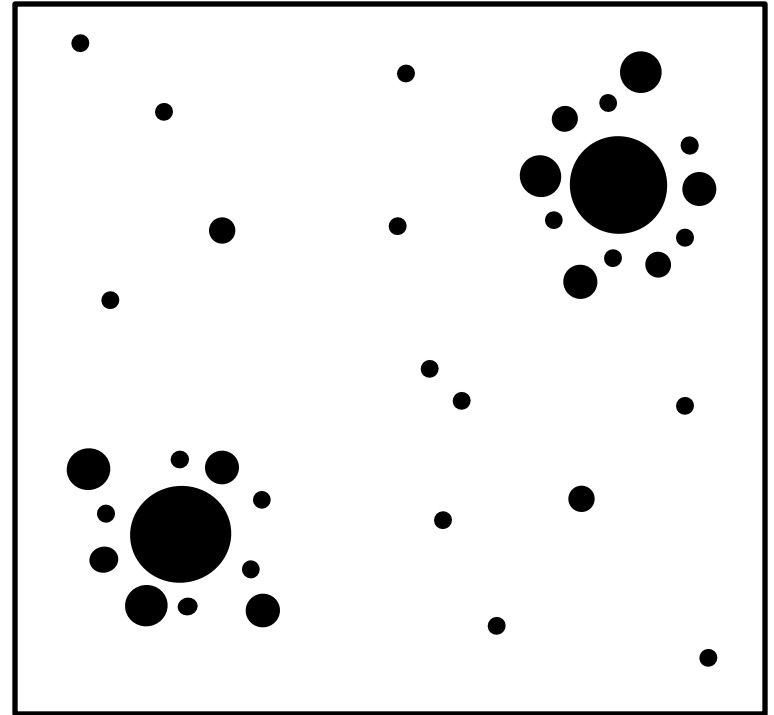
A. Linde (1994)



Spatial Distribution PBH



- Monochromatic
- Uniformly distributed



- Broad range of masses
- PBH in clusters



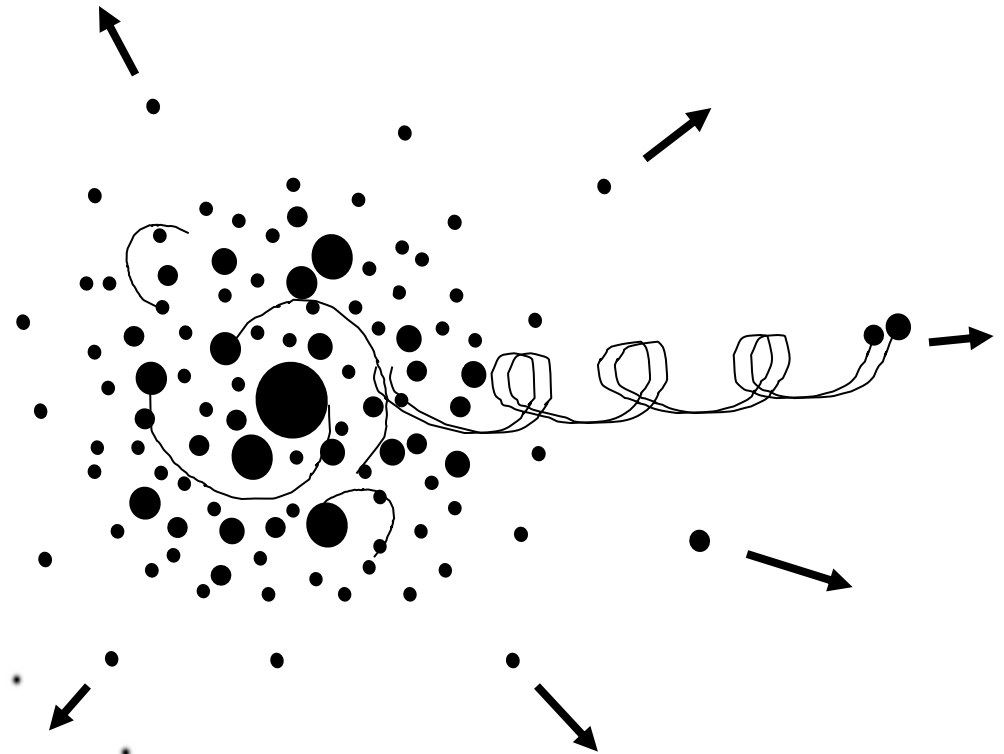
JGB [1702.08275]

Cluster Dynamics

- Initial conditions
- Binary parameter distributions
- Hierarchical mergers (w/ kicks)
- Merger rates
- Spin induction

Cluster Dynamics

Trashorras, JGB, Nesseris [2006.15018]



Cluster Dynamics

J.F. Nuño Siles, JGB [2405.06391]

Lognormal mass distribution

$$N \sim \mathcal{O}(10^3 - 20 \cdot 10^3)$$

$$M_{\text{tot}} \sim \mathcal{O}(10^3 - 10^5) M_{\odot}$$

Maxwellian velocity distribution

Plummer density profile

Galactic potential MW

(point-mass galaxy)

$$M = 4.36953 \times 10^{10} M_{\odot}$$

with circular orbit at $R = 34$ kpc

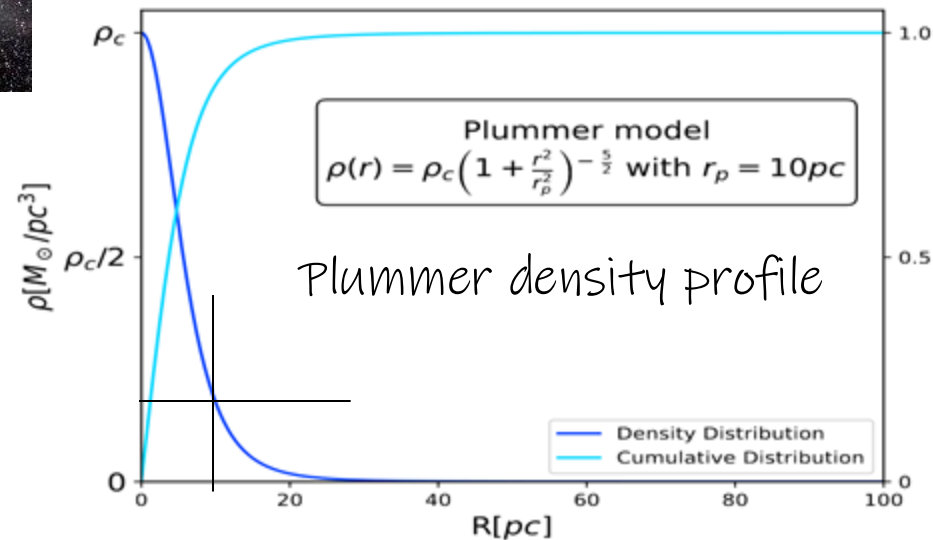
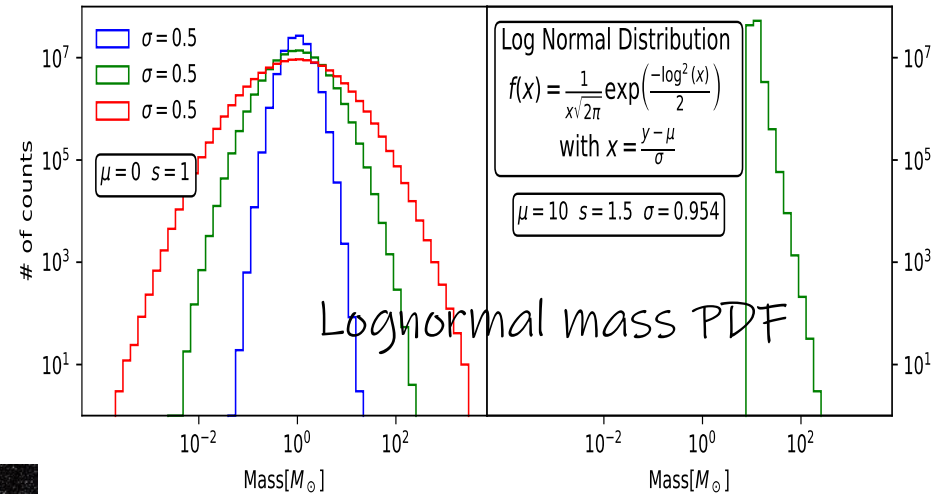
No primordial binaries

Zero natal spin

Code used: [Nbody6++GPU](#)



$\{M\&A, \sigma_{0.5}, \sigma_1, \sigma_{1.5}\}$



Multiple simulations

J.F. Nuño Siles, JGB [2405.06391]

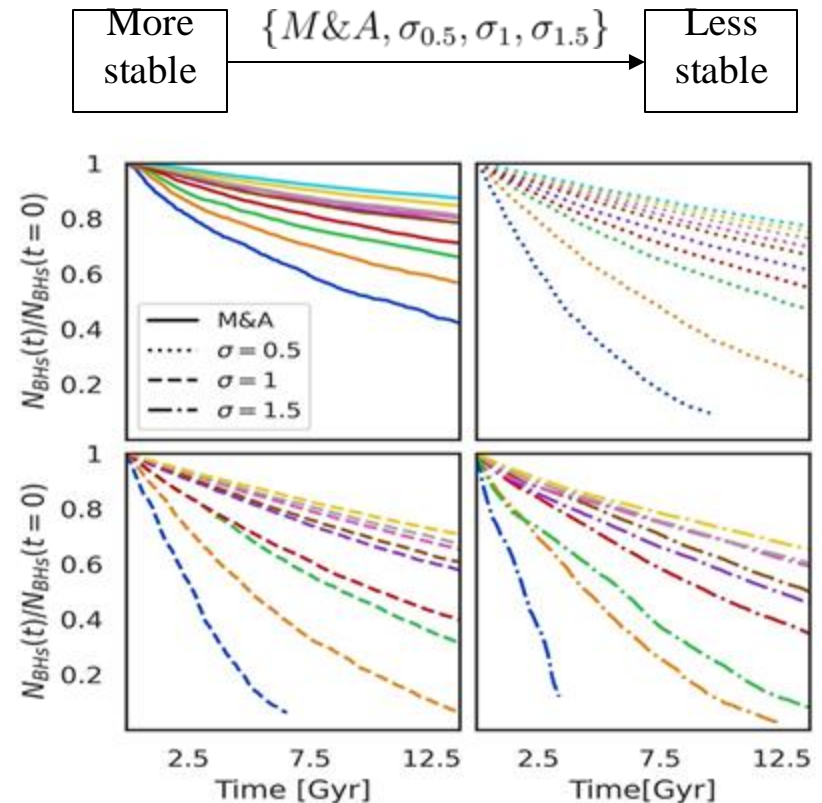
ID M&A	$M_{\text{total}}[M_{\odot}]$ $t = 0$	$M_{\text{max}}[M_{\odot}]$ $t = 0$	$M_{\text{max}}[M_{\odot}]$ $t = T_U$	$R_{\text{HM}}[\text{pc}]$ $t = 0$	$R_{\text{HM}}[\text{pc}]$ $t = T_U$	ID $\sigma_{0.5}$	$M_{\text{total}}[M_{\odot}]$ $t = 0$	$M_{\text{max}}[M_{\odot}]$ $t = 0$	$M_{\text{max}}[M_{\odot}]$ $t = T_U$	$R_{\text{HM}}[\text{pc}]$ $t = 0$	$R_{\text{HM}}[\text{pc}]$ $t = T_U$
1295	16140	46.54	46.54	2.20	27.04	1520	1389	5.03	5.03	9.72	12.25
2570	32166	66.10	97.80	2.38	27.17	3345	3007	4.50	5.08	3.23	15.55
4046	50088	63.64	91.98	4.27	26.74	5480	5009	6.67	6.67	0.77	16.21
5199	64280	69.98	74.80	2.20	28.39	7678	7008	5.69	7.52	1.92	15.15
8077	100116	78.27	78.27	12.53	29.50	9937	9001	5.48	5.48	1.25	15.85
8922	110196	76.15	81.52	13.31	32.01	12201	11001	5.00	7.77	2.90	15.29
10372	128337	104.26	104.26	6.20	27.54	14366	13005	5.42	8.22	2.65	16.04
10535	130198	68.50	74.35	9.72	28.20	16428	14912	7.72	7.72	0.48	16.04
16159	200392	57.75	113.59	4.44	27.24	18776	17007	5.40	6.51	2.29	15.00
20738	256346	134.10	145.70	1.37	26.65	20866	18918	5.31	7.36	3.91	15.35
ID σ_1	$M_{\text{total}}[M_{\odot}]$ $t = 0$	$M_{\text{max}}[M_{\odot}]$ $t = 0$	$M_{\text{max}}[M_{\odot}]$ $t = T_U$	$R_{\text{HM}}[\text{pc}]$ $t = 0$	$R_{\text{HM}}[\text{pc}]$ $t = T_U$	ID $\sigma_{1.5}$	$M_{\text{total}}[M_{\odot}]$ $t = 0$	$M_{\text{max}}[M_{\odot}]$ $t = 0$	$M_{\text{max}}[M_{\odot}]$ $t = T_U$	$R_{\text{HM}}[\text{pc}]$ $t = 0$	$R_{\text{HM}}[\text{pc}]$ $t = T_U$
1505	2003	32.07	32.07	1.93	27.07	1220	3020	63.67	63.67	3.37	58.92
3090	4004	18.56	18.56	7.52	22.21	3423	8010	105.74	105.74	7.15	41.00
5288	7007	34.14	34.14	7.60	21.97	5258	13014	541.18	541.18	1.95	40.15
7507	10001	25.82	34.29	3.95	24.77	8025	20021	157.23	157.23	0.41	41.62
10663	14000	46.77	46.77	6.64	26.96	10011	24187	179.83	280.36	1.45	60.33
12834	17004	32.81	58.06	4.41	23.91	12409	30007	114.51	114.51	0.07	55.98
15136	20000	58.31	58.31	0.47	25.47	14691	38027	731.69	1004.13	1.40	37.81
17554	23008	45.68	64.90	0.82	25.62	17182	43013	554.27	554.27	5.59	46.36
20590	27008	51.60	76.41	4.70	26.64	20261	49021	657.47	784.02	3.52	41.41

Cluster Dynamics

J.F. Nuño Siles, JGB [2405.06391]

All the clusters are metastable or directly unstable, that is, they dissolved in a time comparable with the age of the Universe or will do so in the future

Some types of clusters are more stable than others, depending on the mass ratio distribution of the pairwise interactions.



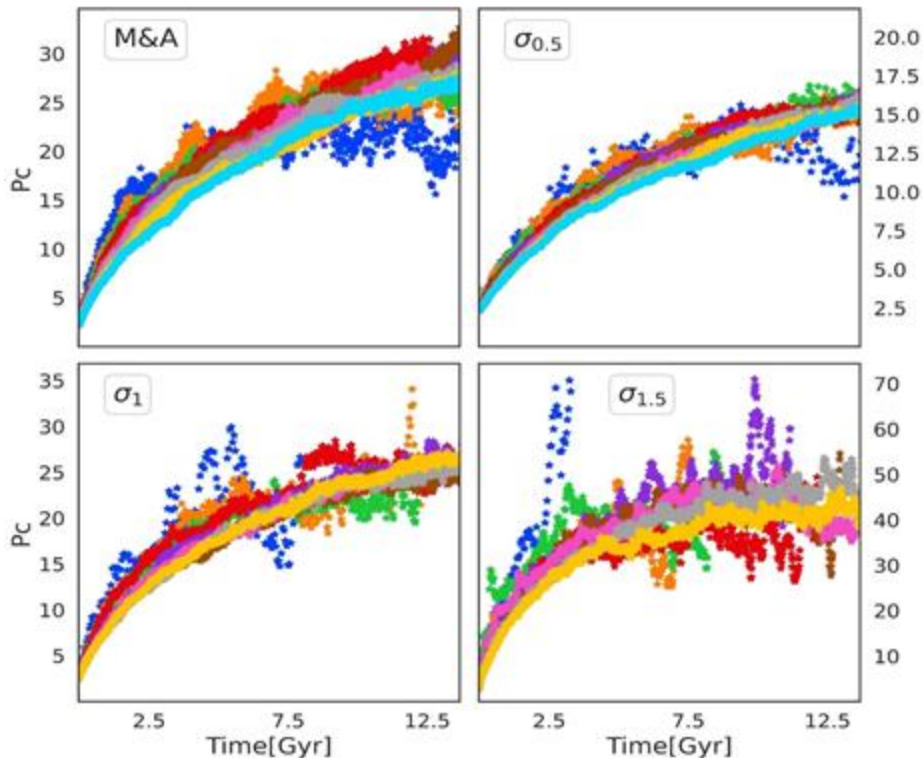
BHs remaining in clusters within 13.6 Gyr

Cluster Dynamics

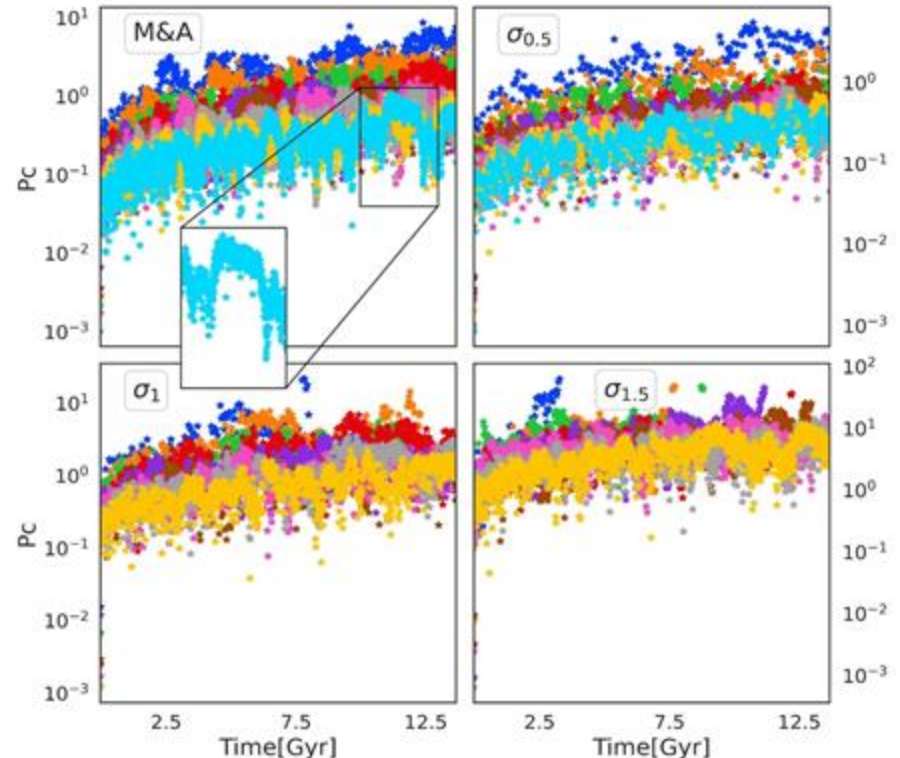
Clusters expand with time while core radius stays almost constant

JFN+JGB [2405.06391]

$R_{HM}(t)$



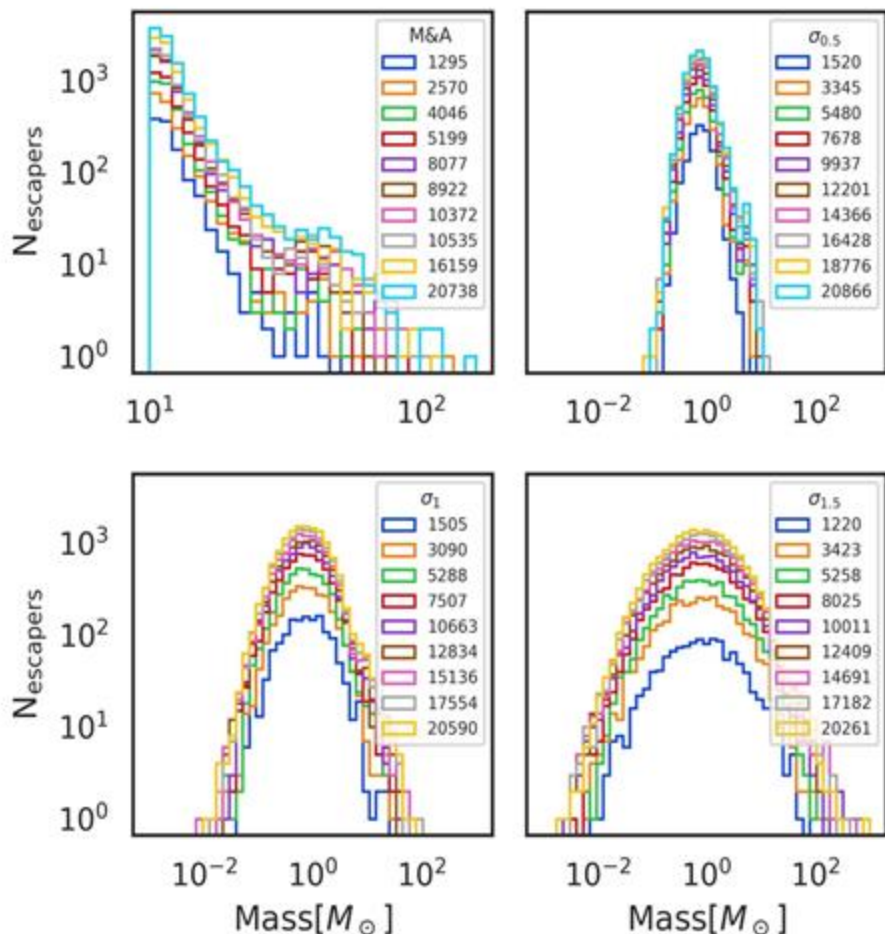
$R_c(t)$



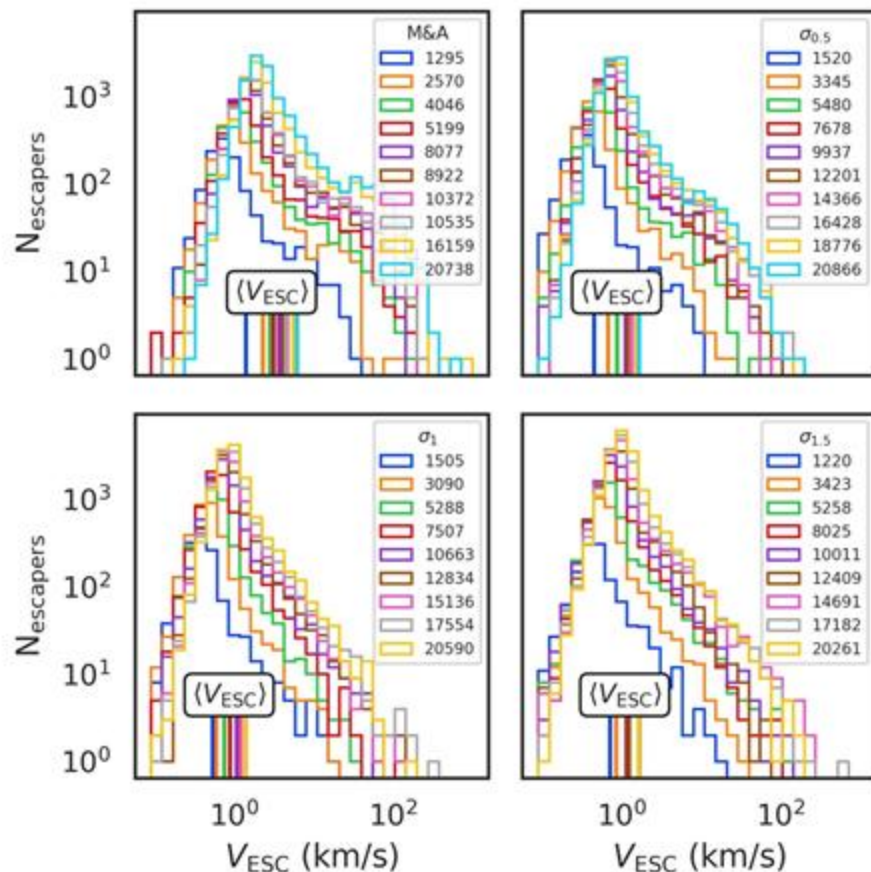
Distribution of escapers

JFN+JGB [2405.06391]

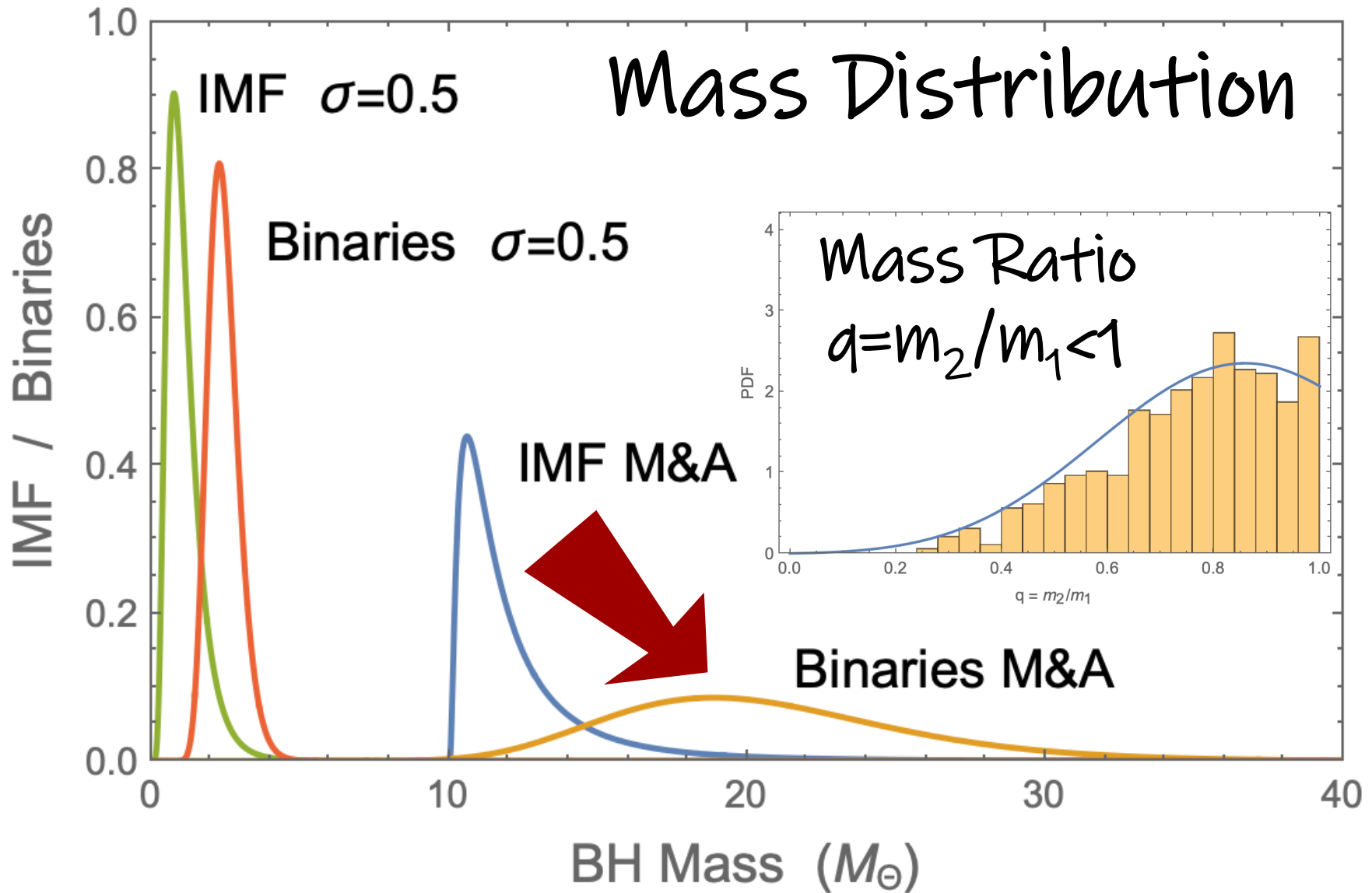
Mass



Escape velocity



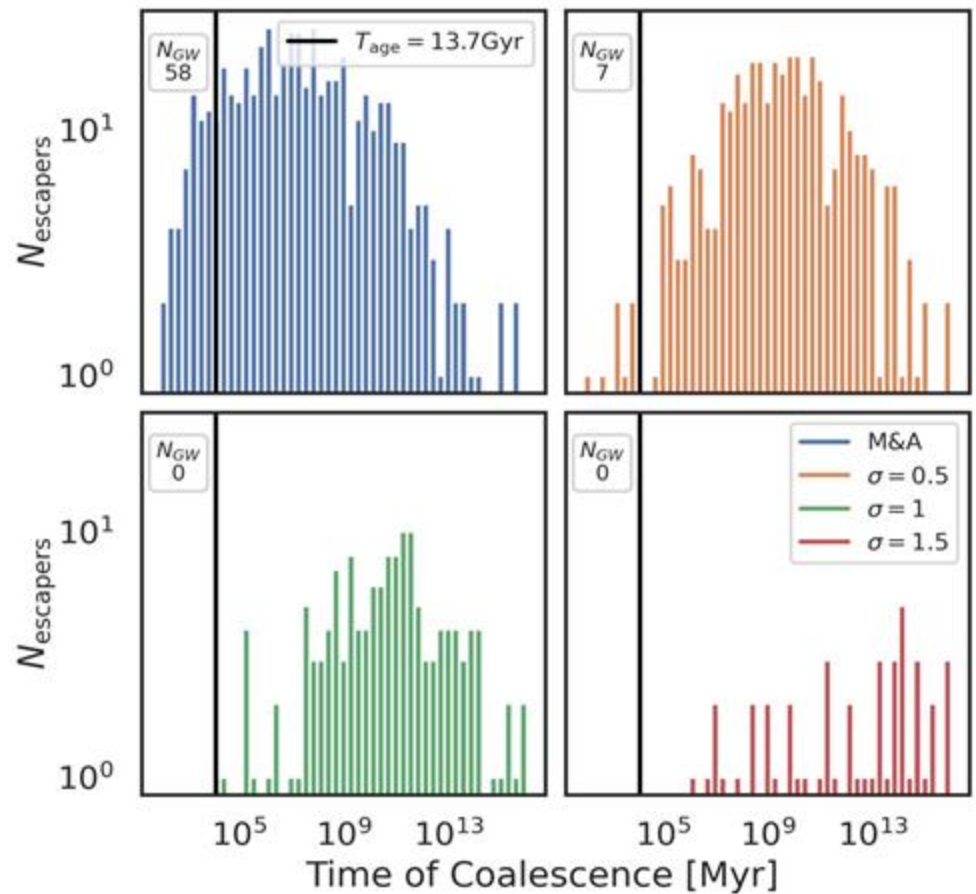
Binary escapers



Binary escapers

- The larger the initial N , the harder the binary needs to be to escape.
- Mainly highly eccentric (at birth) binaries coalesce in a Hubble time.
- Most binaries would not have merged by now. Only $\{58, 7, 0, 0\}$ of the $\{504, 371, 153, 60\}$ binary escapers are off-cluster mergers within the age of the universe.
- Binary escapers merger rate lognormal in time

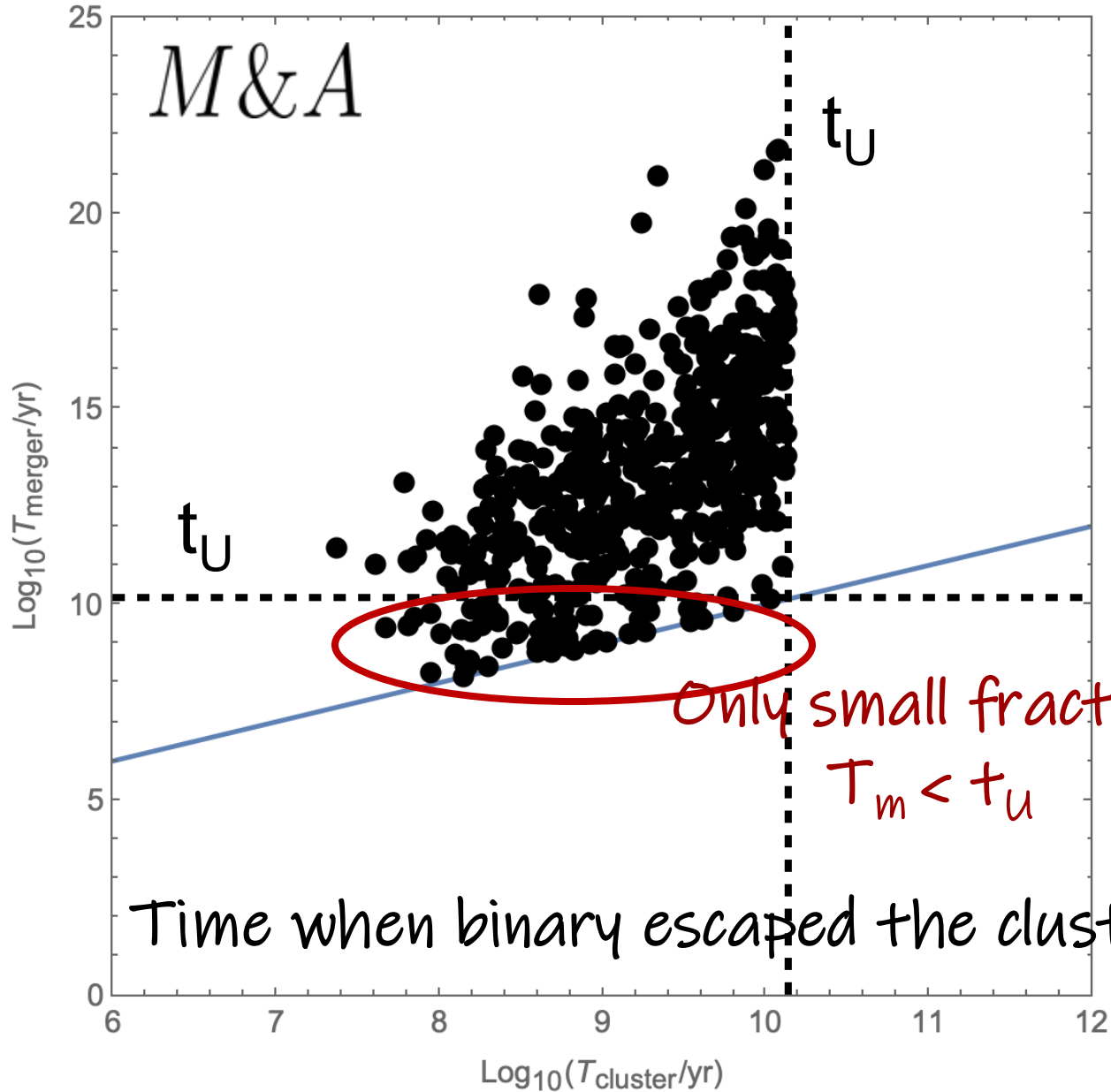
JFN+JGB [2405.06391]



Distribution of merger times for binary escapers using the quasi-circular orbit approximation

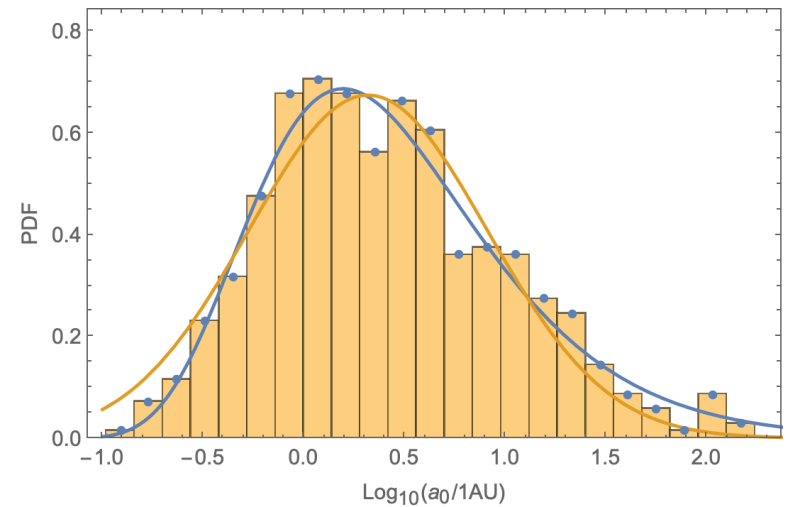
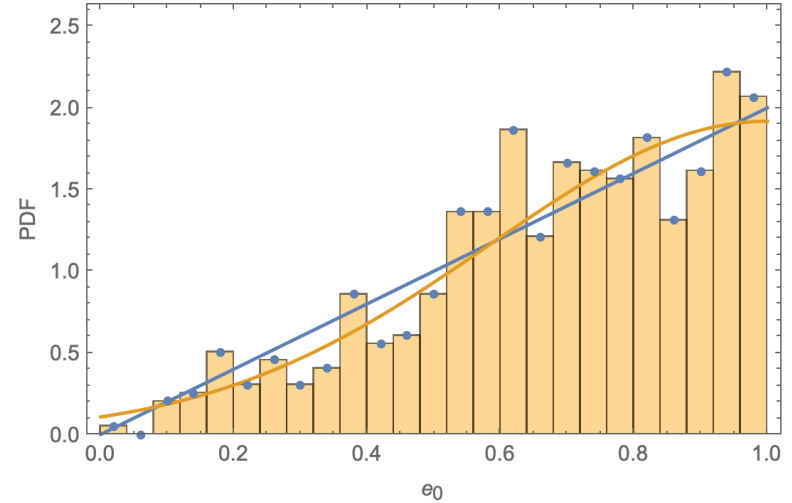
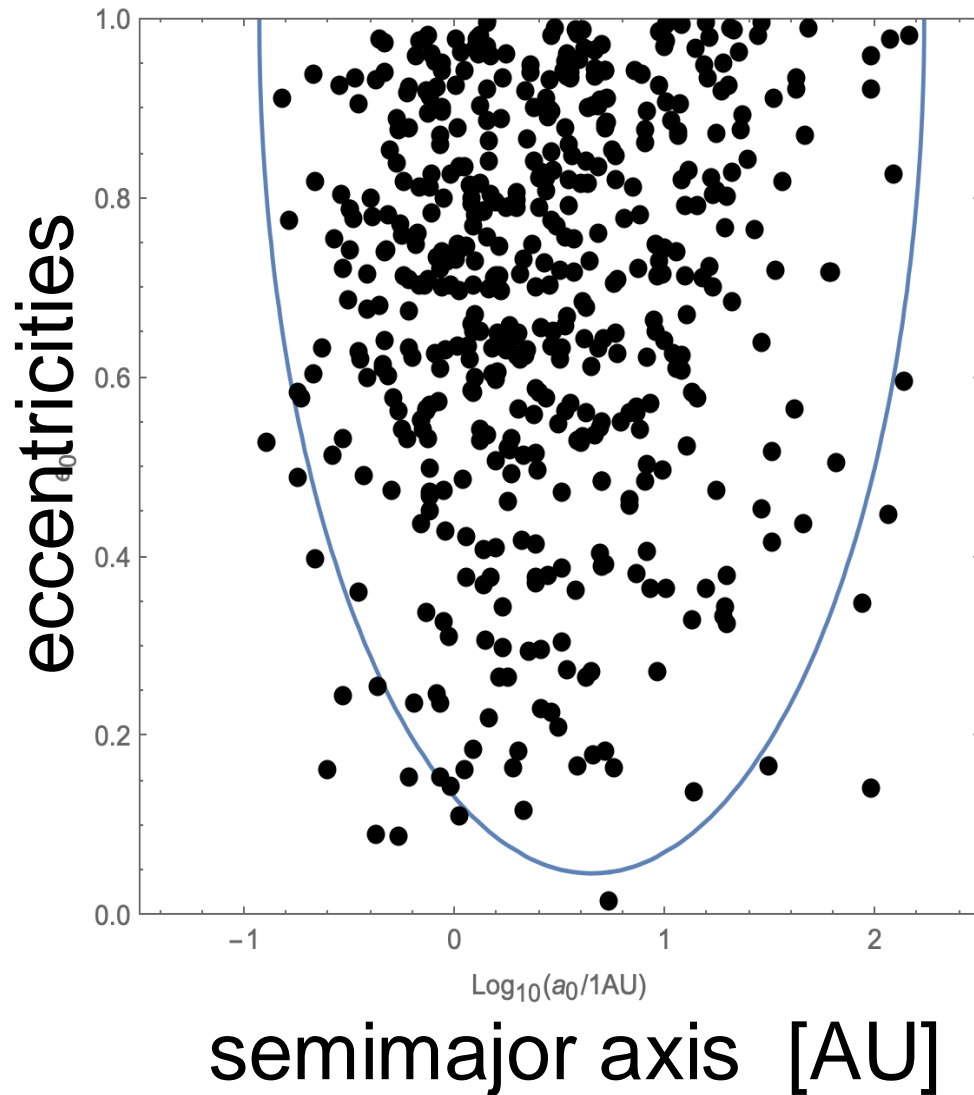
Binary escapers

Time when escaped binary merged



Binary escapers

M&A

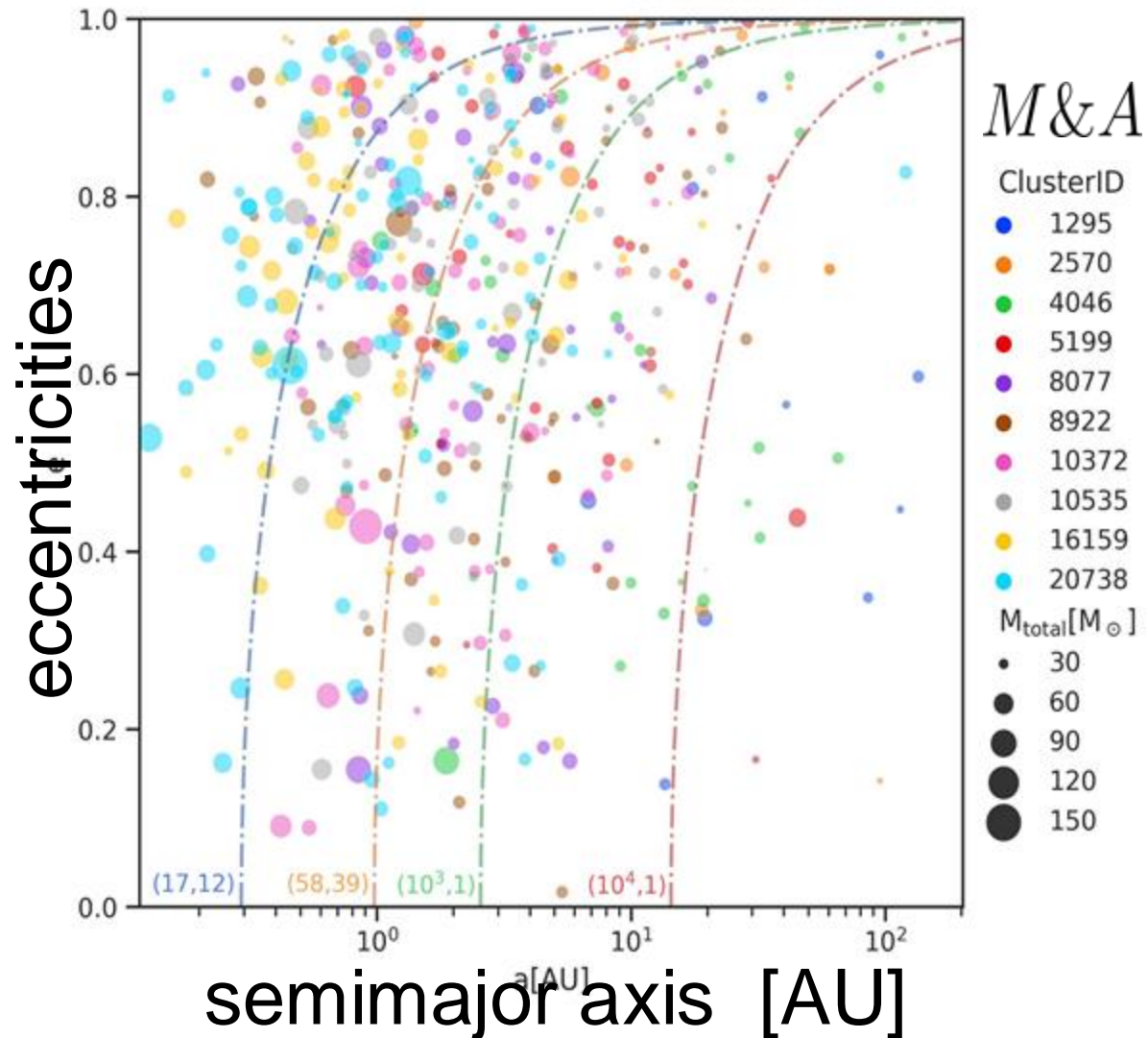


Binary escapers

Numbers increase with initial density but ratio decreases

The larger the initial N , the smaller the semimajor axis of the binaries, that is, the harder the binary.

Mainly highly eccentric binaries coalesce in a Hubble time

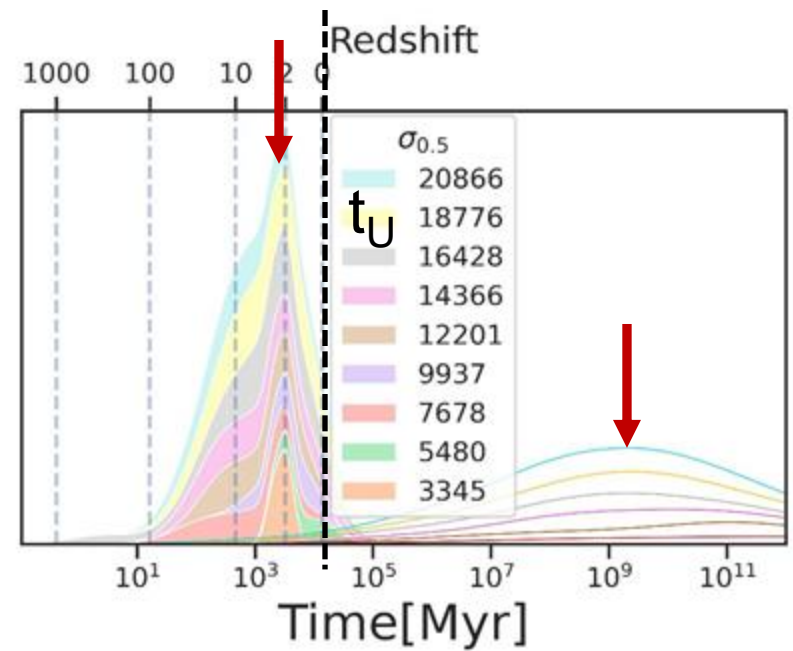
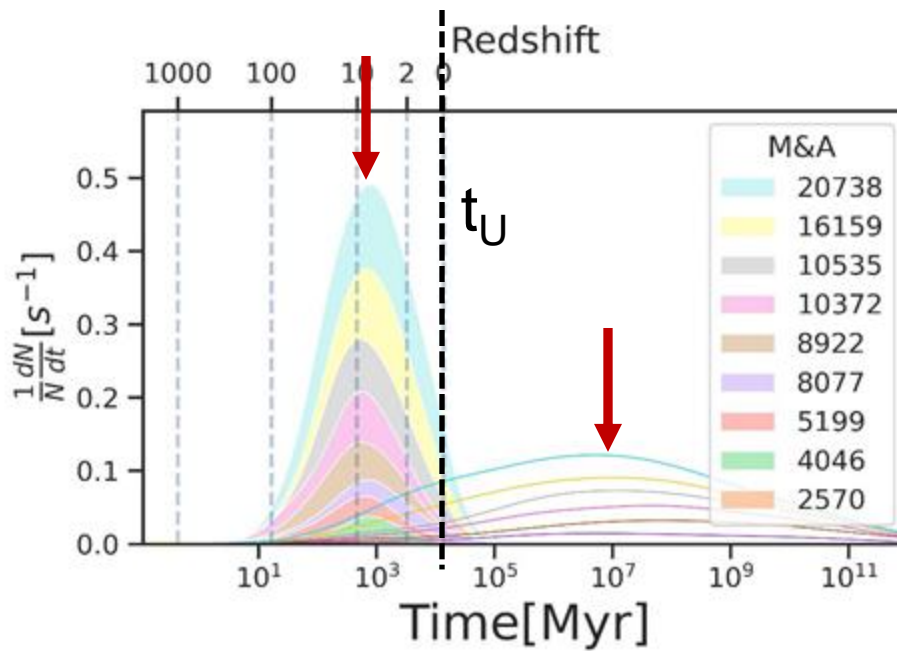


Distribution of eccentricities and semimajor axes of the binary escapers.

BBH merger rates

In-cluster merger rate
for $\sigma_{0.5}$ peaks at $z \sim 8$
for M&A peaks at $z \sim 2$

Escapers merger rate
 $\sigma_{0.5}$ peaks at $10^3 t_U$
M&A peaks at $10^5 t_U$

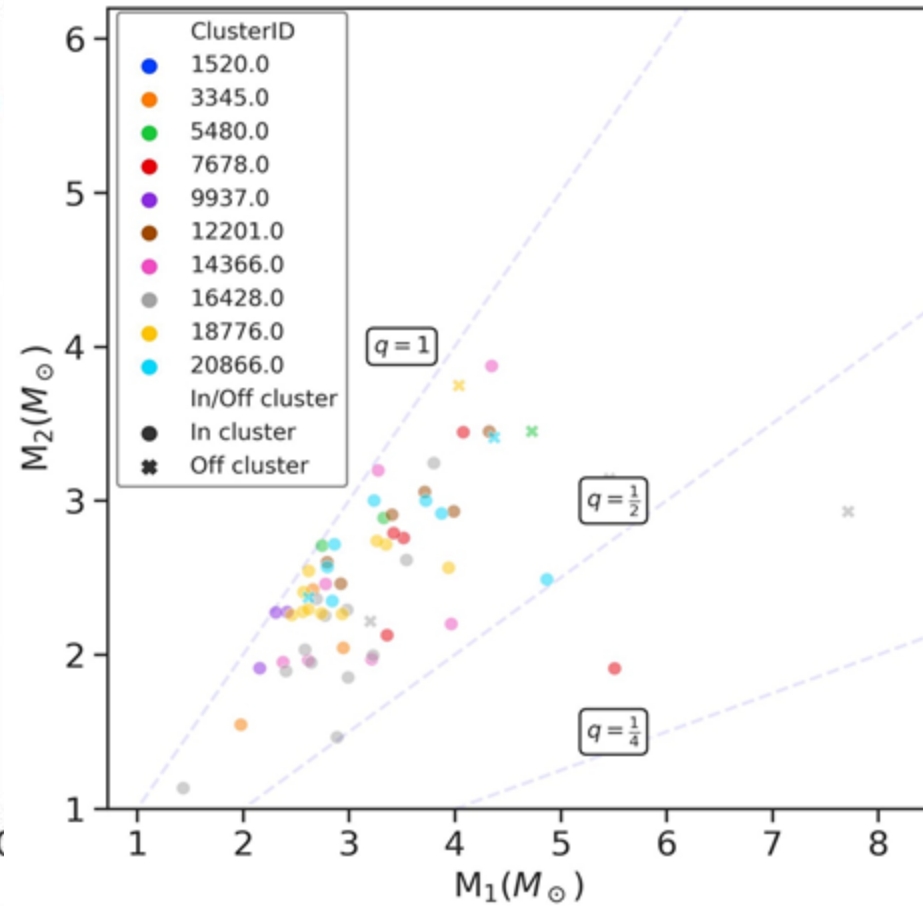
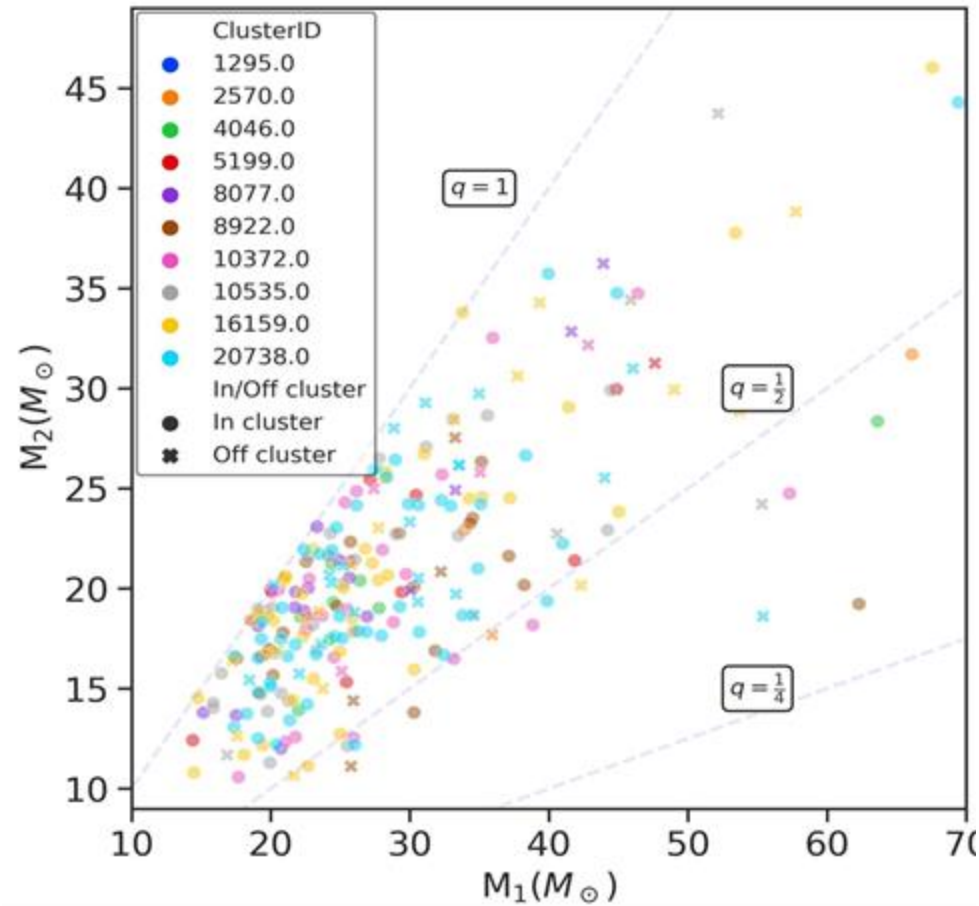


In-cluster and binary escapers merger rate

BBH merger masses

$M \& A$

$\sigma_{0.5}$



Distribution of the masses (m_1 , m_2) of the BBHs mergers

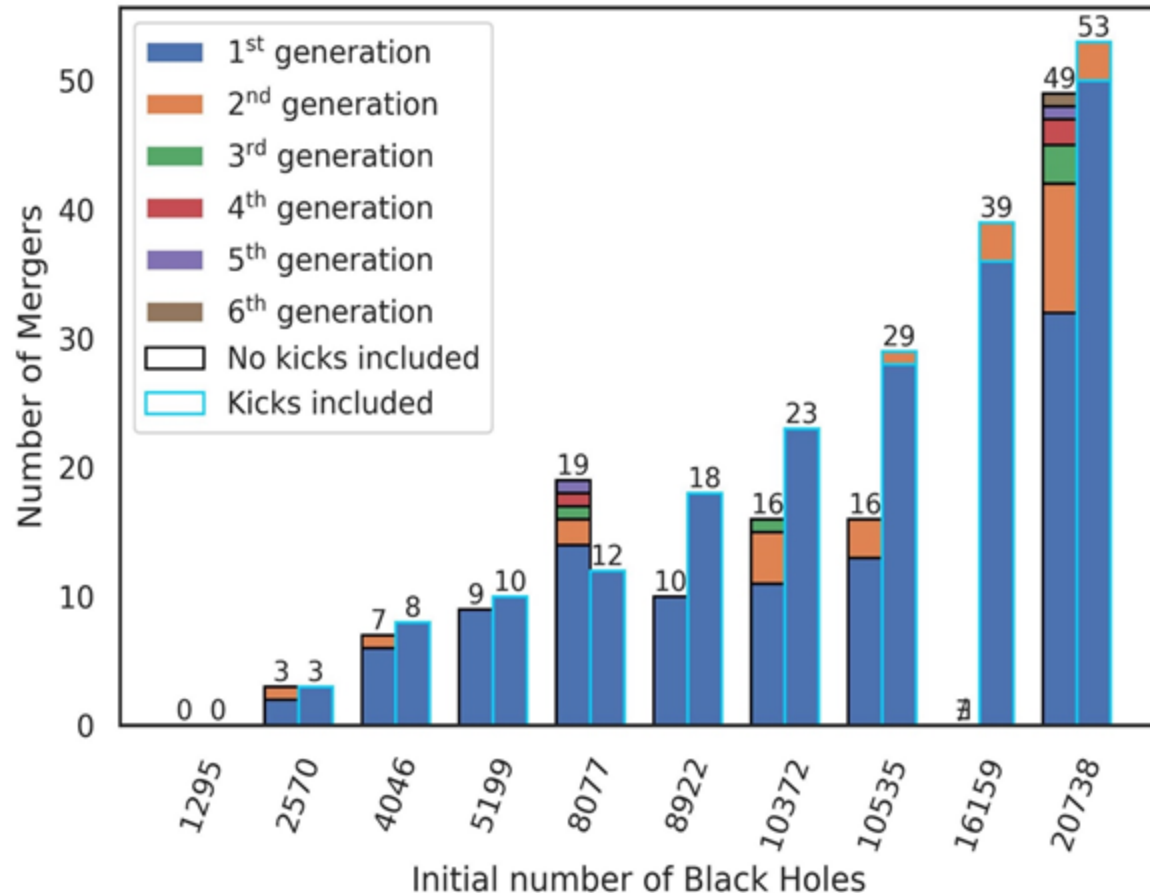
BBH merger kicks

M&A

Best environment to study and understand implications as collisions are numerous

BH kicks as implemented in **Nbody6++GPU** based on Campanelli et al.

Probability of hierarchical mergers drastically reduced



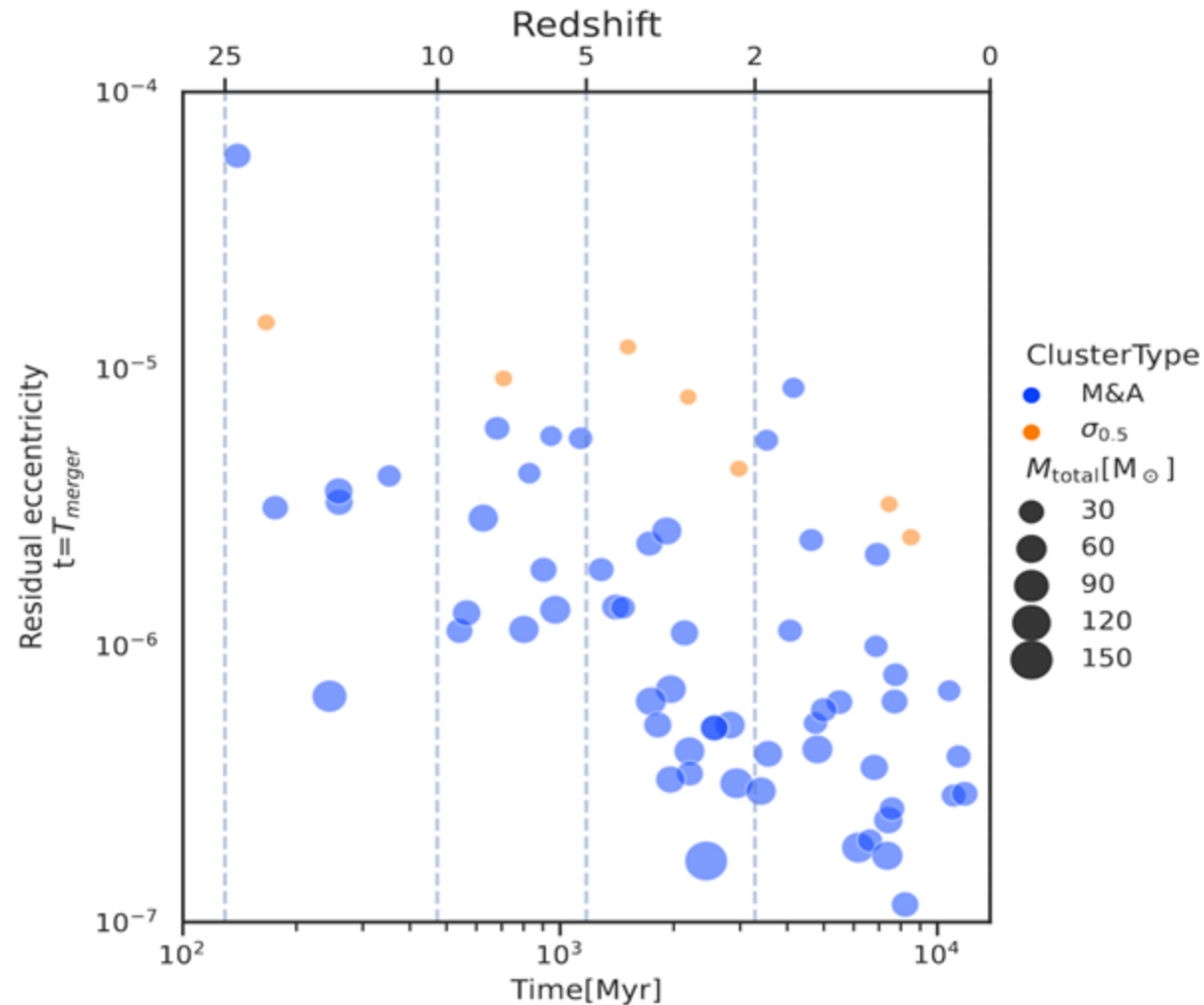
Histogram of the number of in-cluster mergers for the *M&A* type with and without considering BH kicks

BBH merger eccent.'s

GW searches assume quasi-circular approx. How good is this hypothesis?

Residual eccentricity less than 10^{-4} at $f=10\text{Hz}$

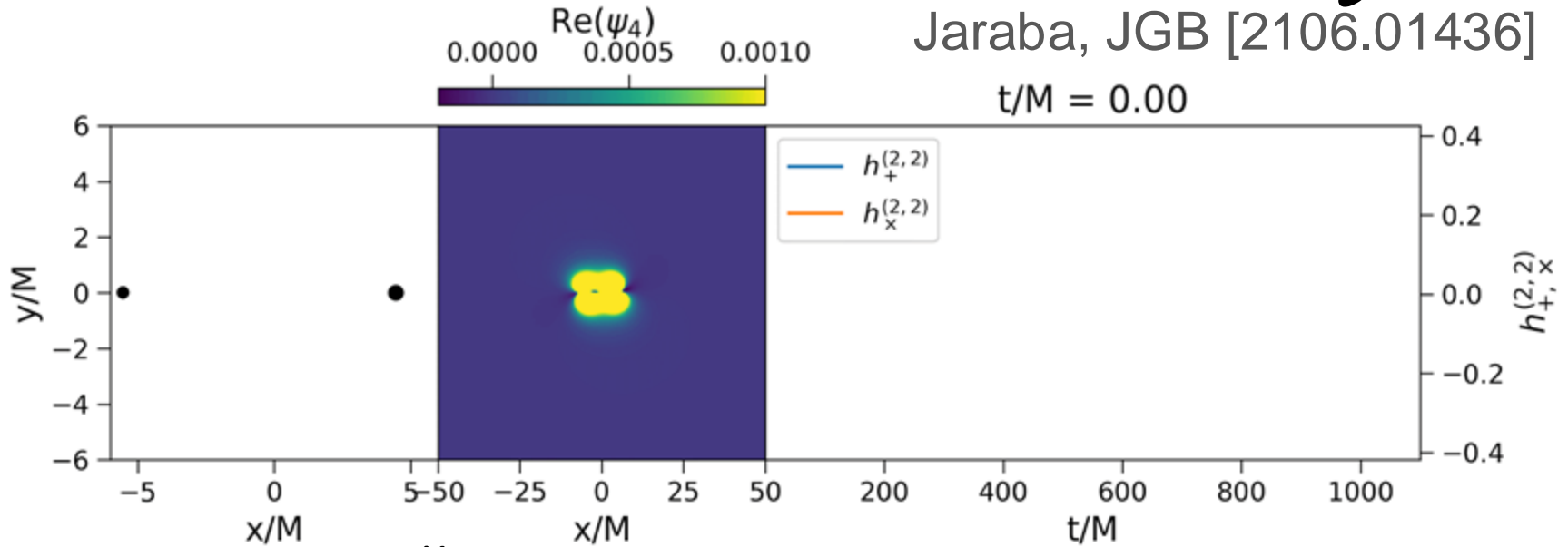
Uncorrelated with redshift



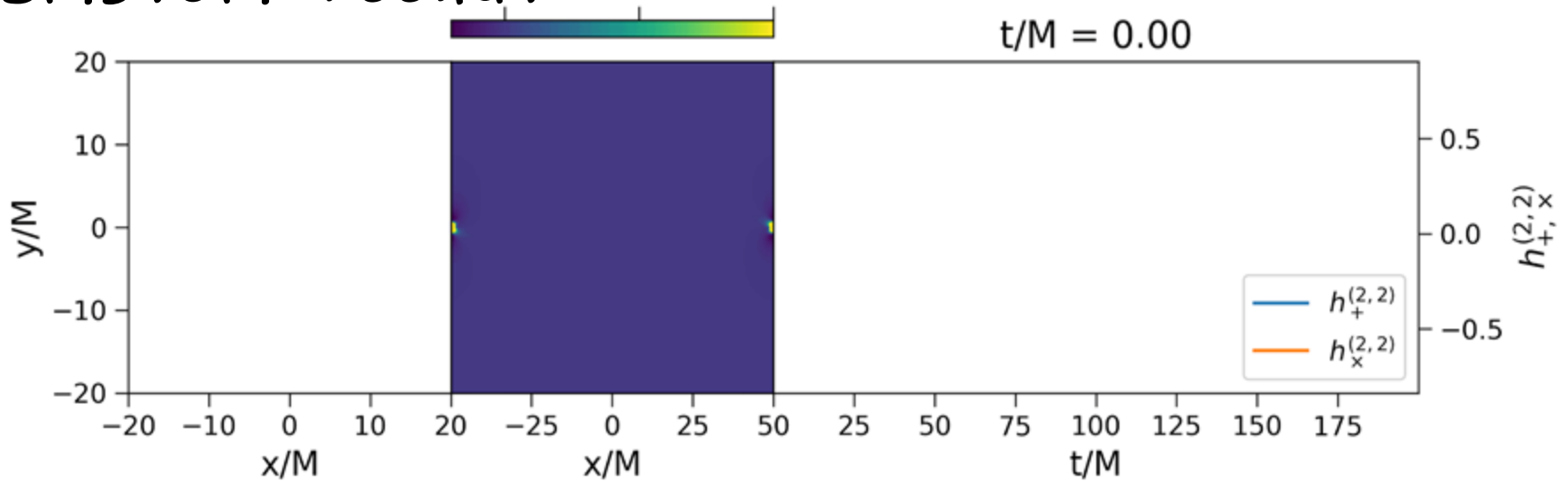
Residual eccentricity of the off-cluster mergers

Inspirals vs scatterings

Jaraba, JGB [2106.01436]

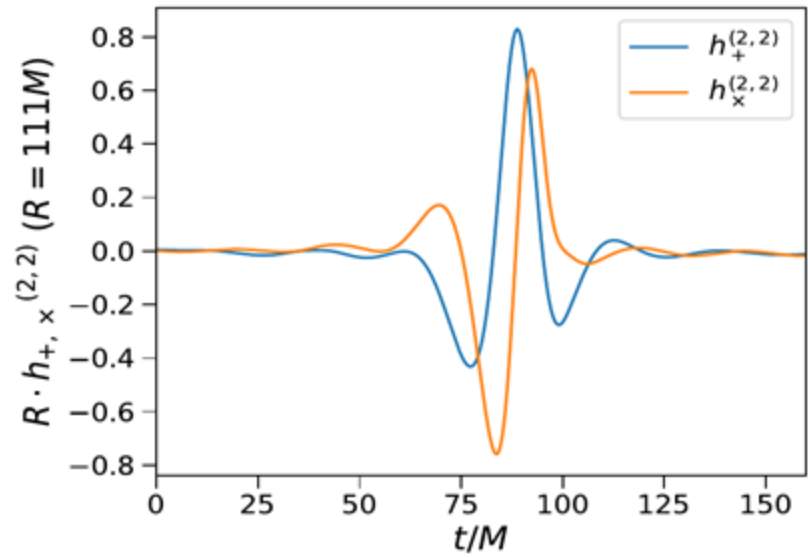
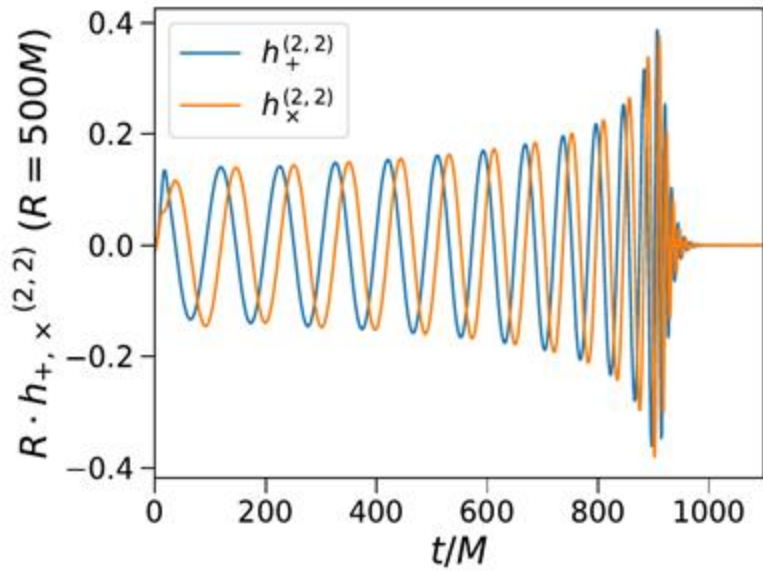


Einstein Toolkit



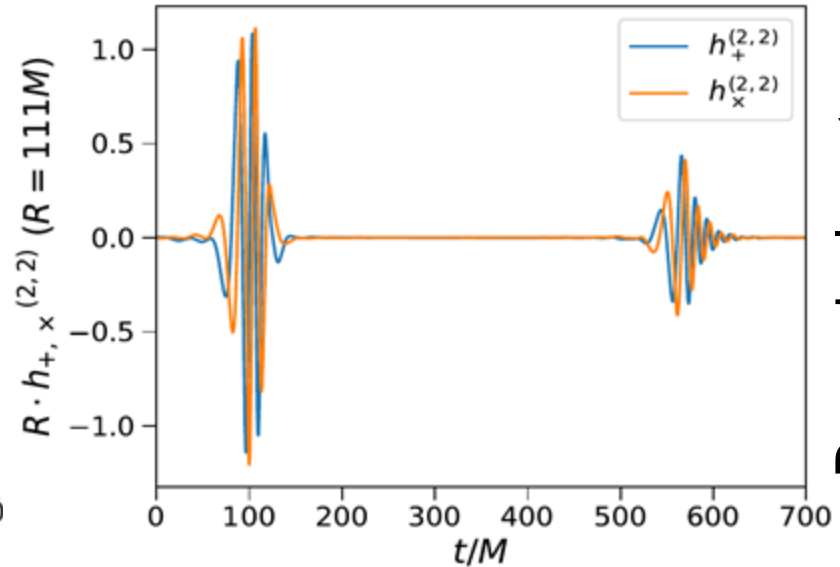
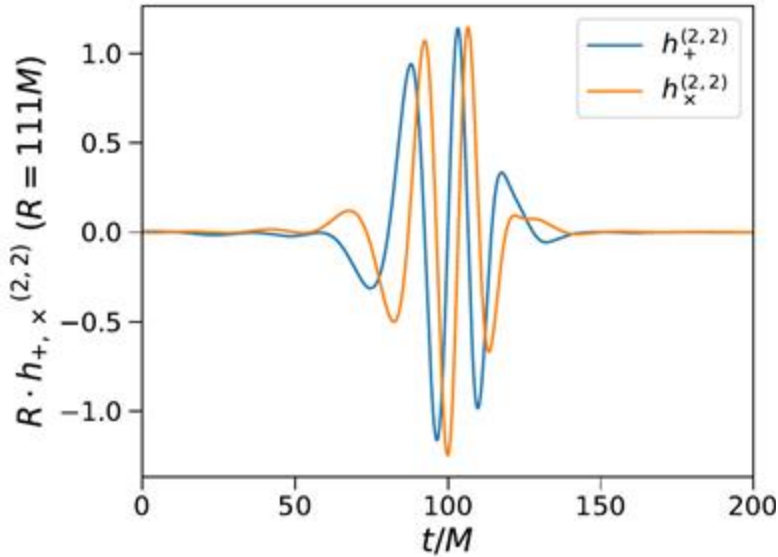
Inspirals vs scatterings

CBC (GW150914)



CHE ($d/M=100, q=1,$
 $p/M=0.49, \theta=4.01^\circ$)

CHE ($d/M=100, q=1,$
 $p/M=0.49, \theta=3.12^\circ$)

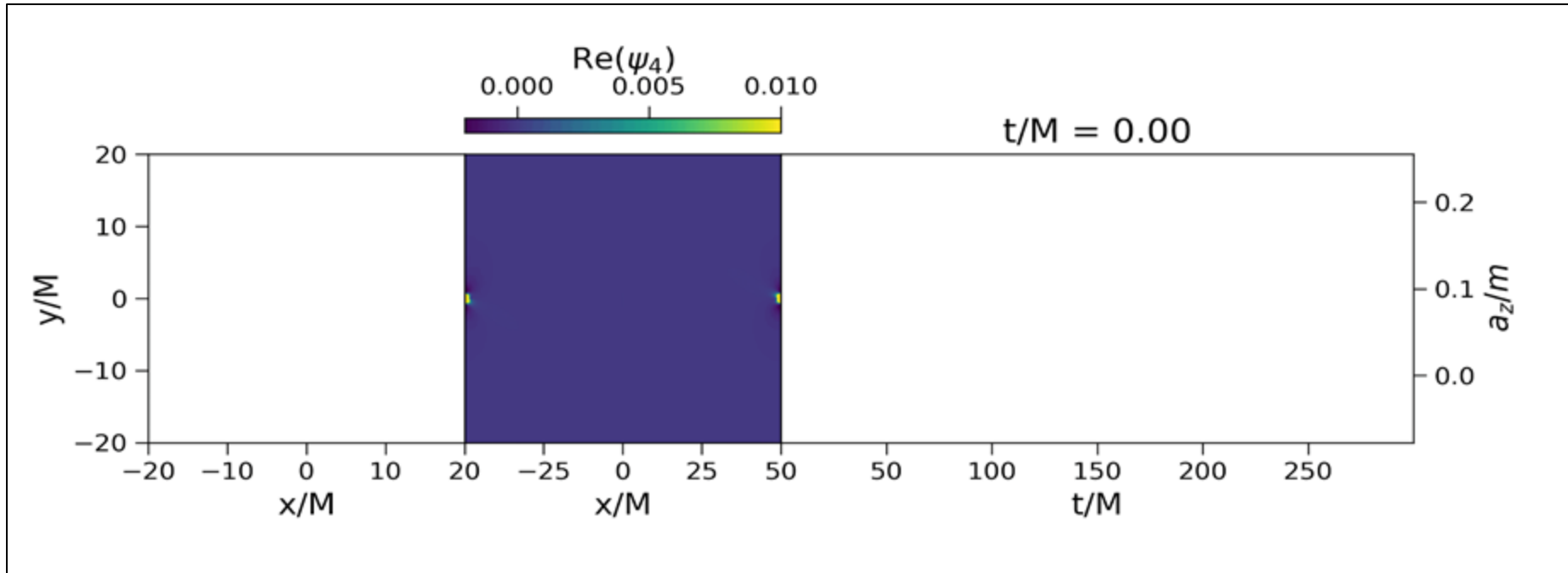
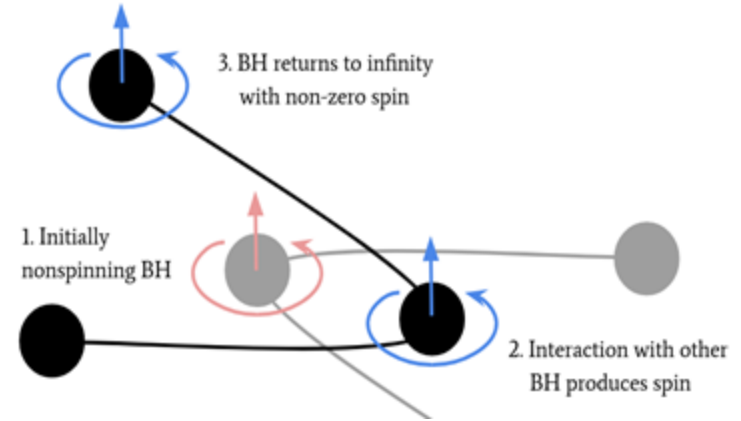


Dynamical capture
($d/M=100, q=1, p/M=0.49,$
 $\theta=3.11^\circ$)

Spin induction in dense clusters

Spin acquired at periastron, during GW emission.

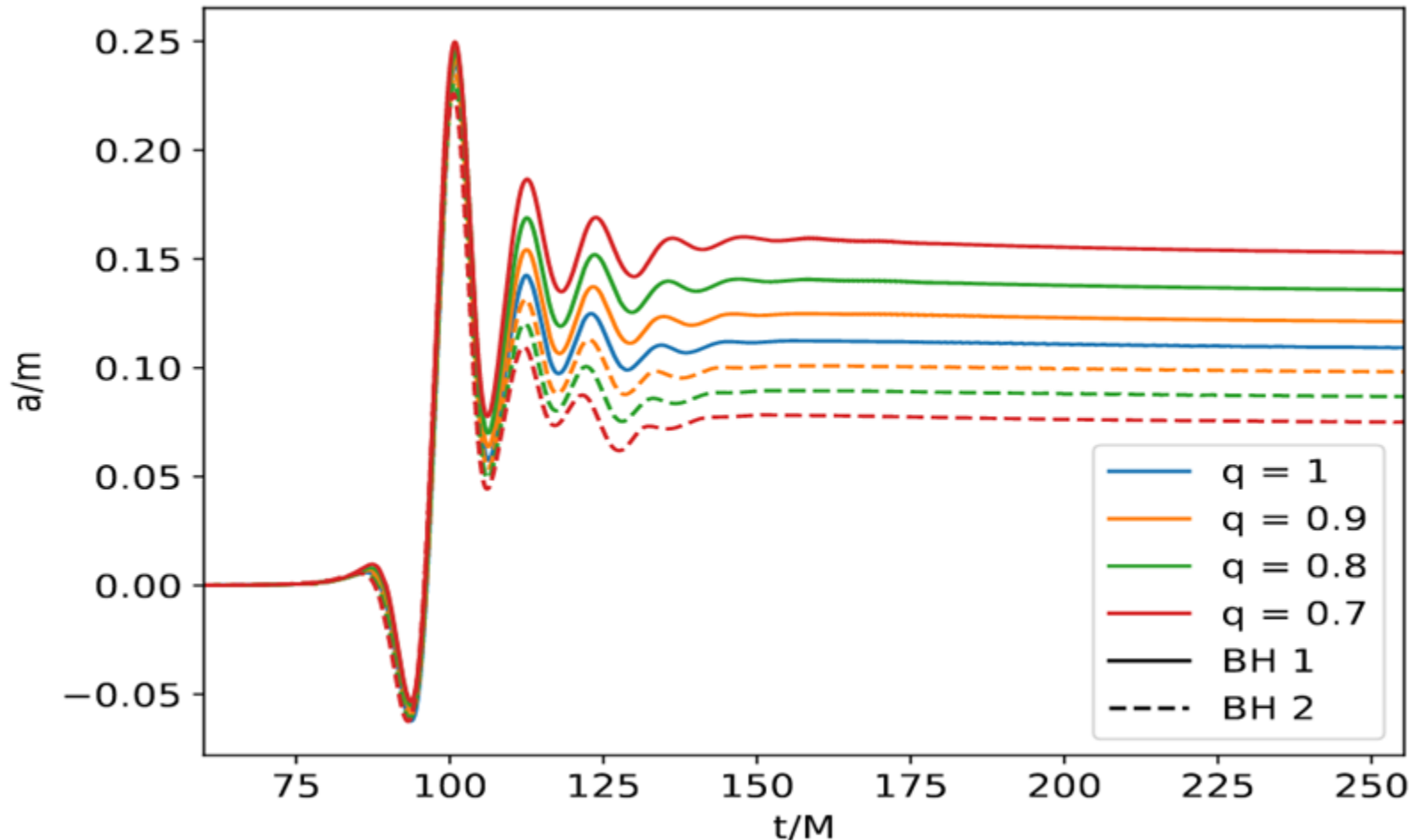
Characterized by Kerr parameter a .



Spin induction in dense clusters

Highest spin is induced in most massive black hole. $q = m_2/m_1 \leq 1$.

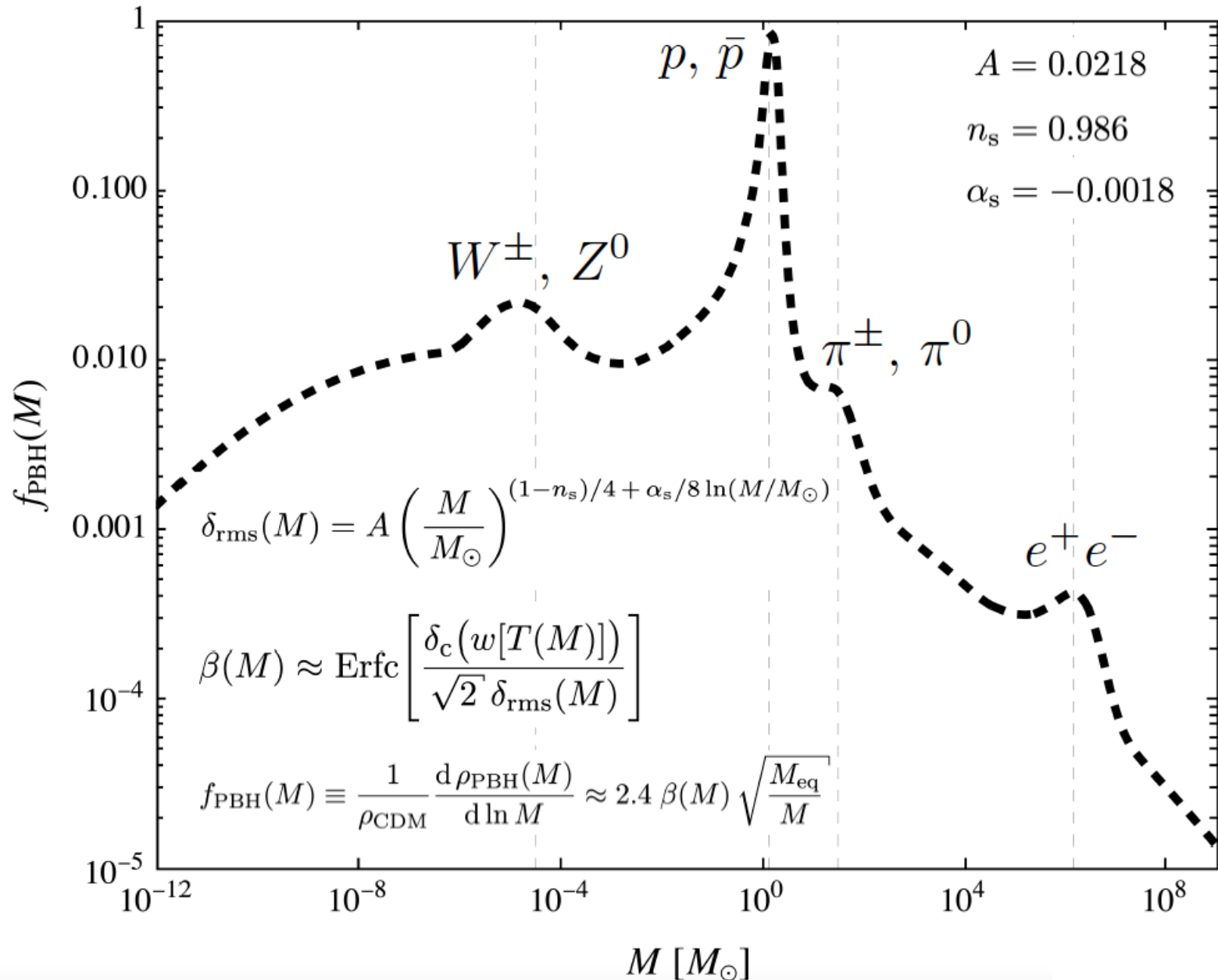
Spin induction is enhanced for the massive black hole when $q \ll 1$.



Observational Evidences

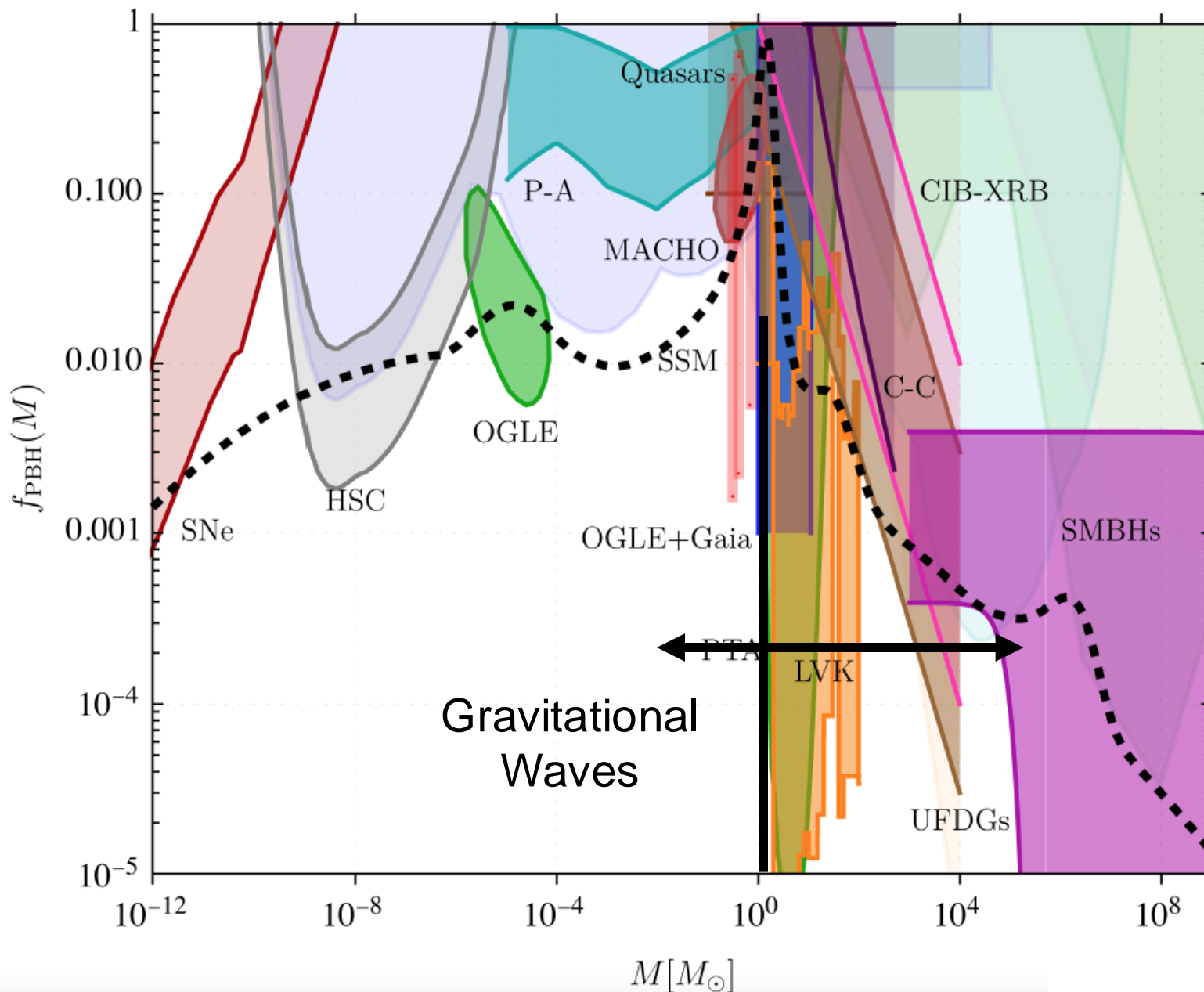
Observational evidence for primordial black holes

Carr, Clesse, JGB, Hawkins, Kühnel [2306.03903]

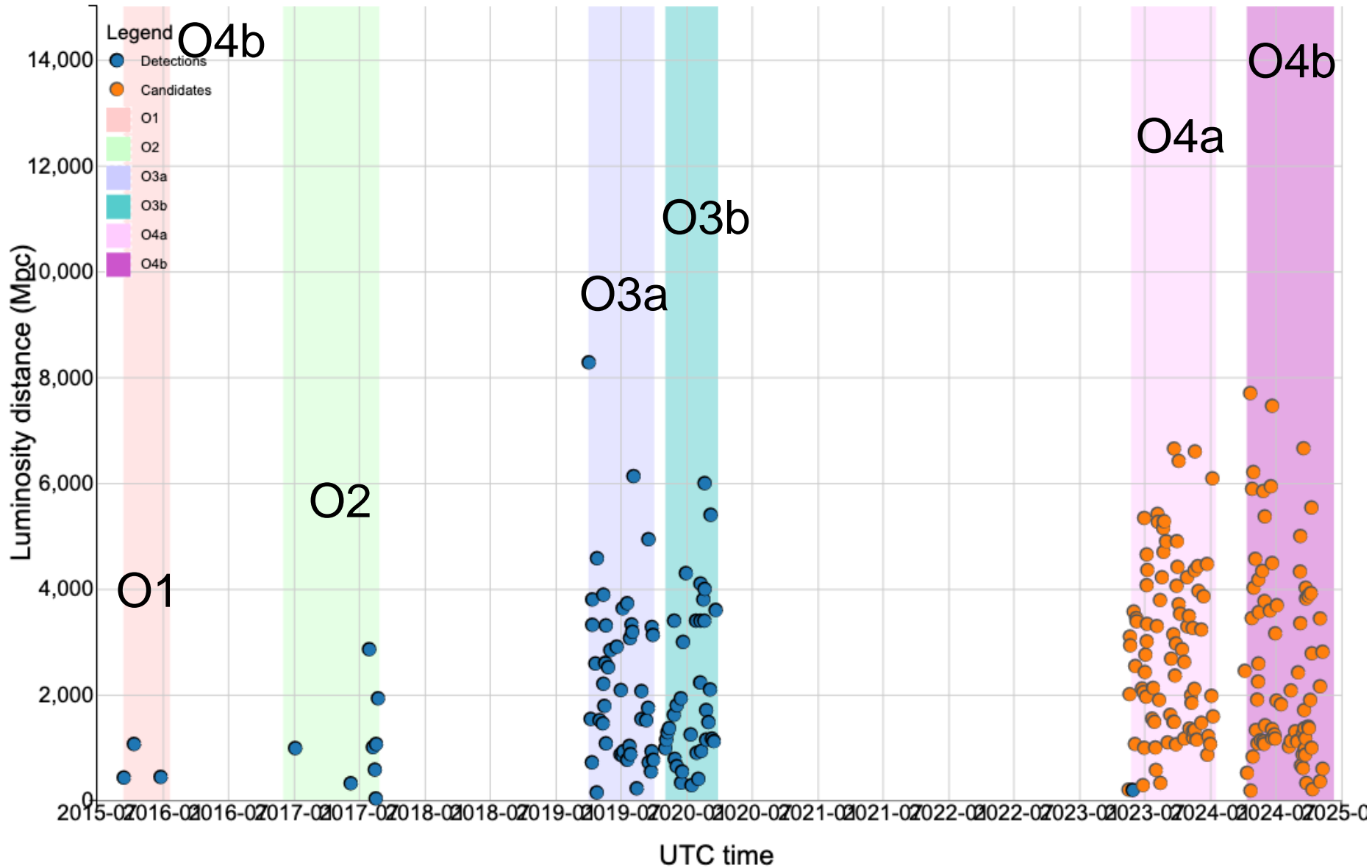


Observational evidence for primordial black holes

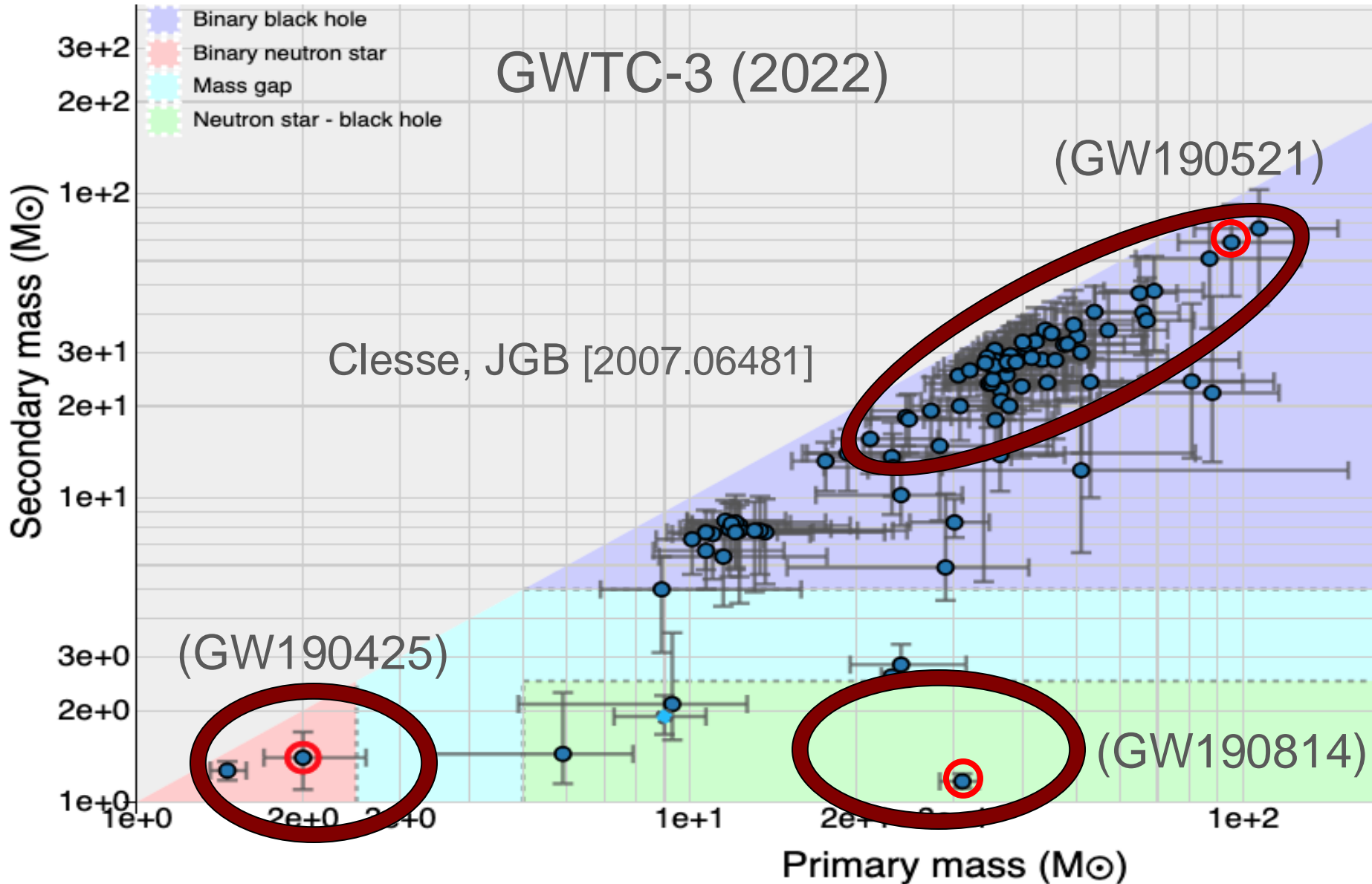
Carr, Clesse, JGB, Hawkins, Kühnel [2306.03903]



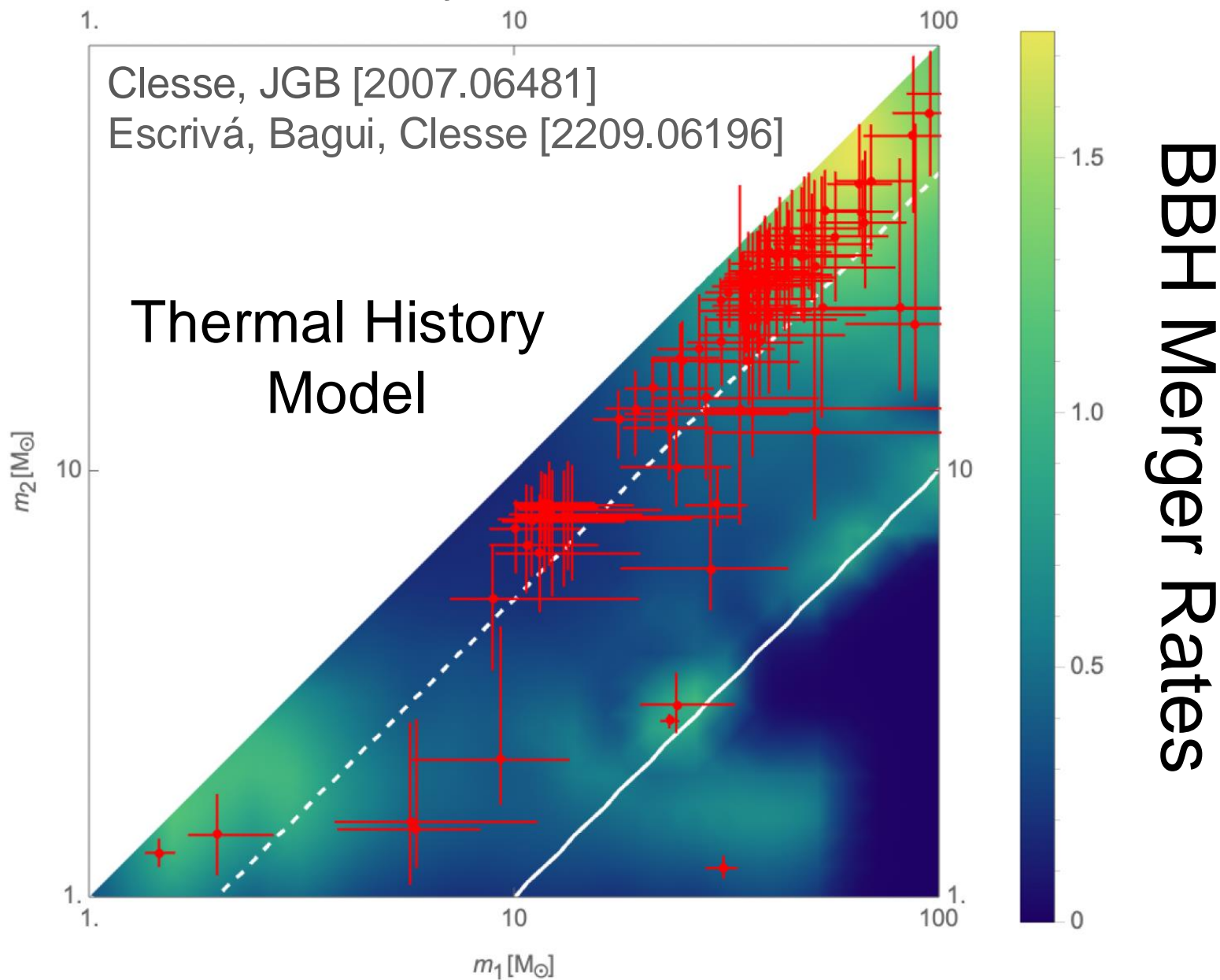
GWTC-1/4 LVK Coll. (2024)



Primary and secondary masses

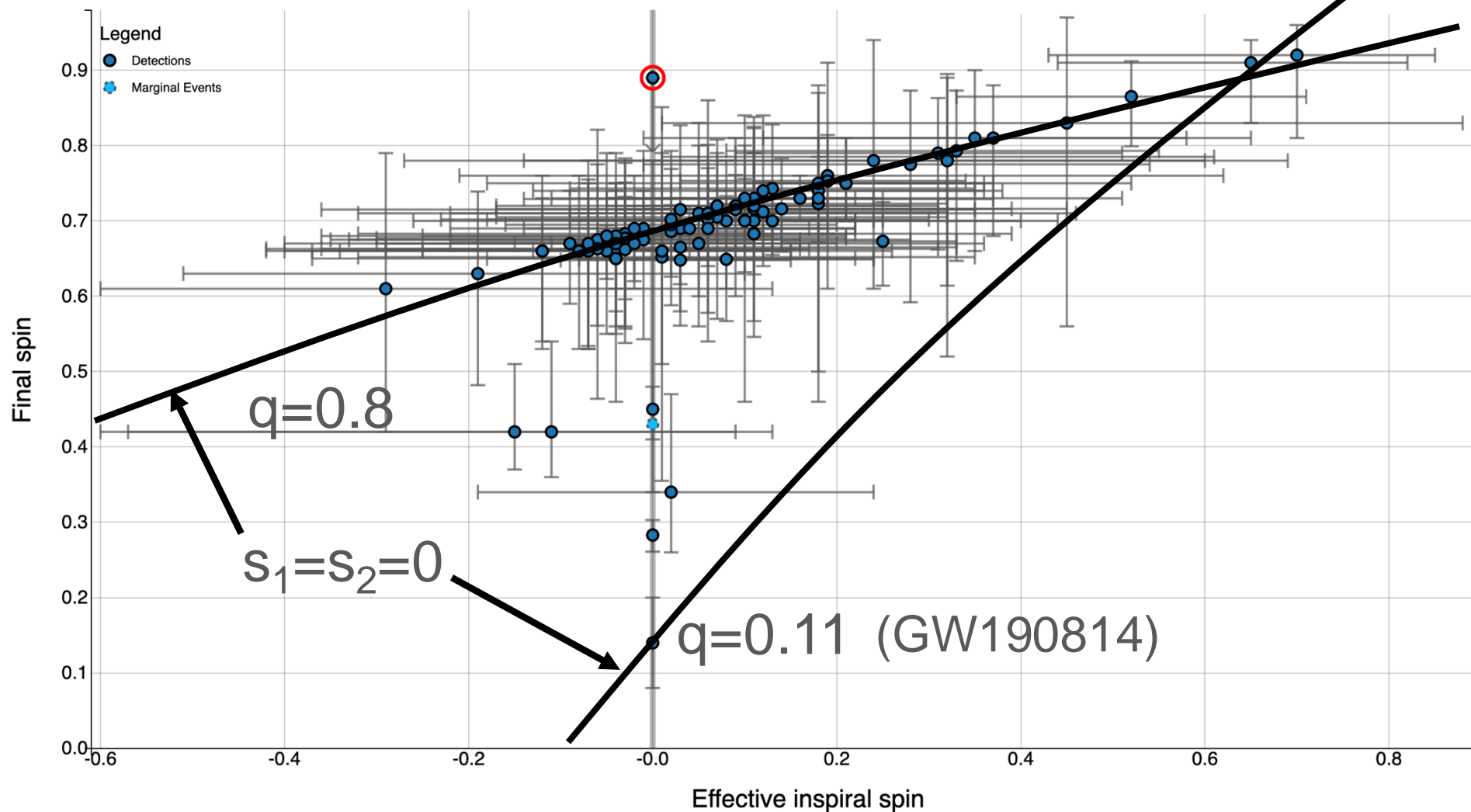


Are LIGO/Virgo BH Primordial?



Effective and Final Spin

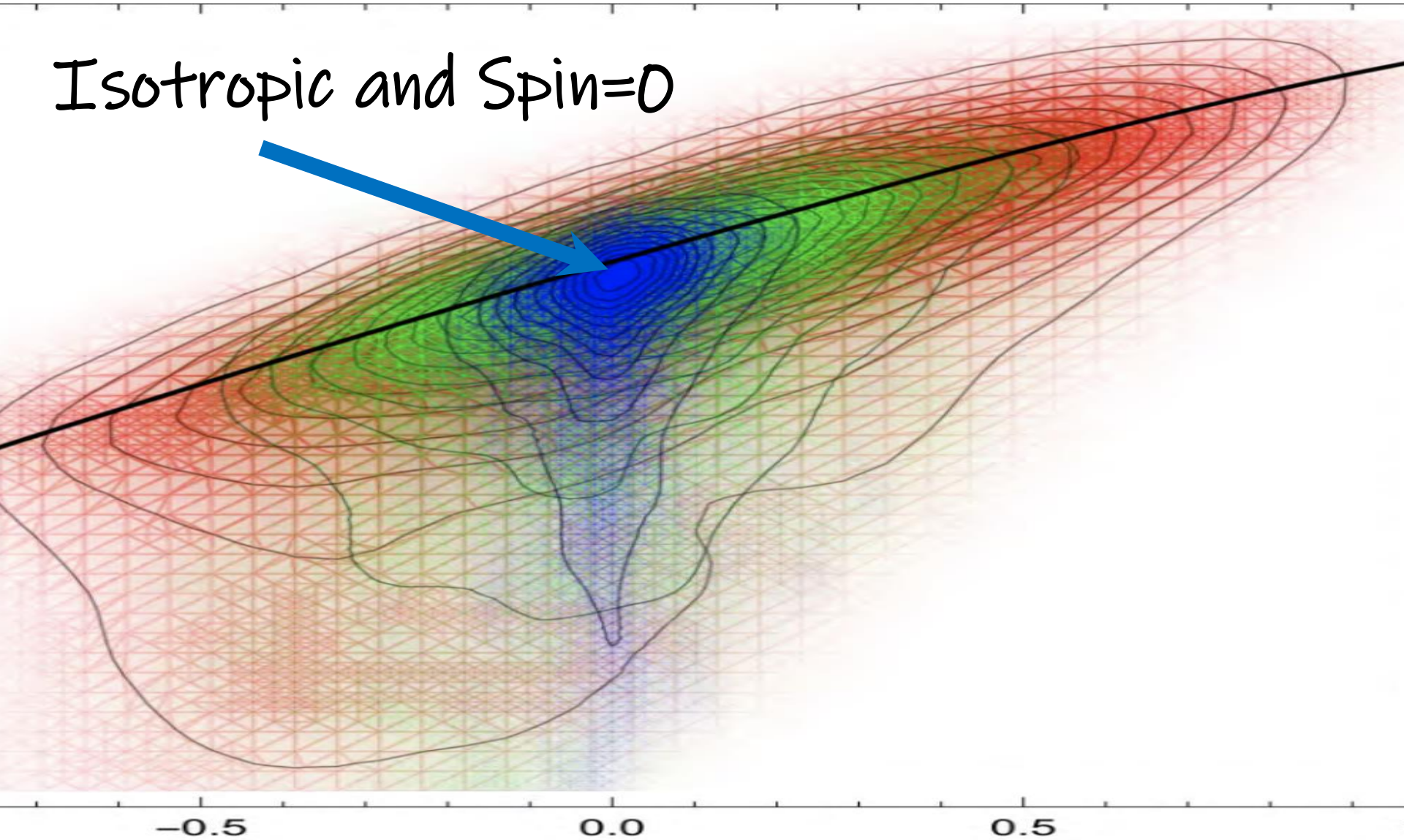
GWTC-3 (2022)



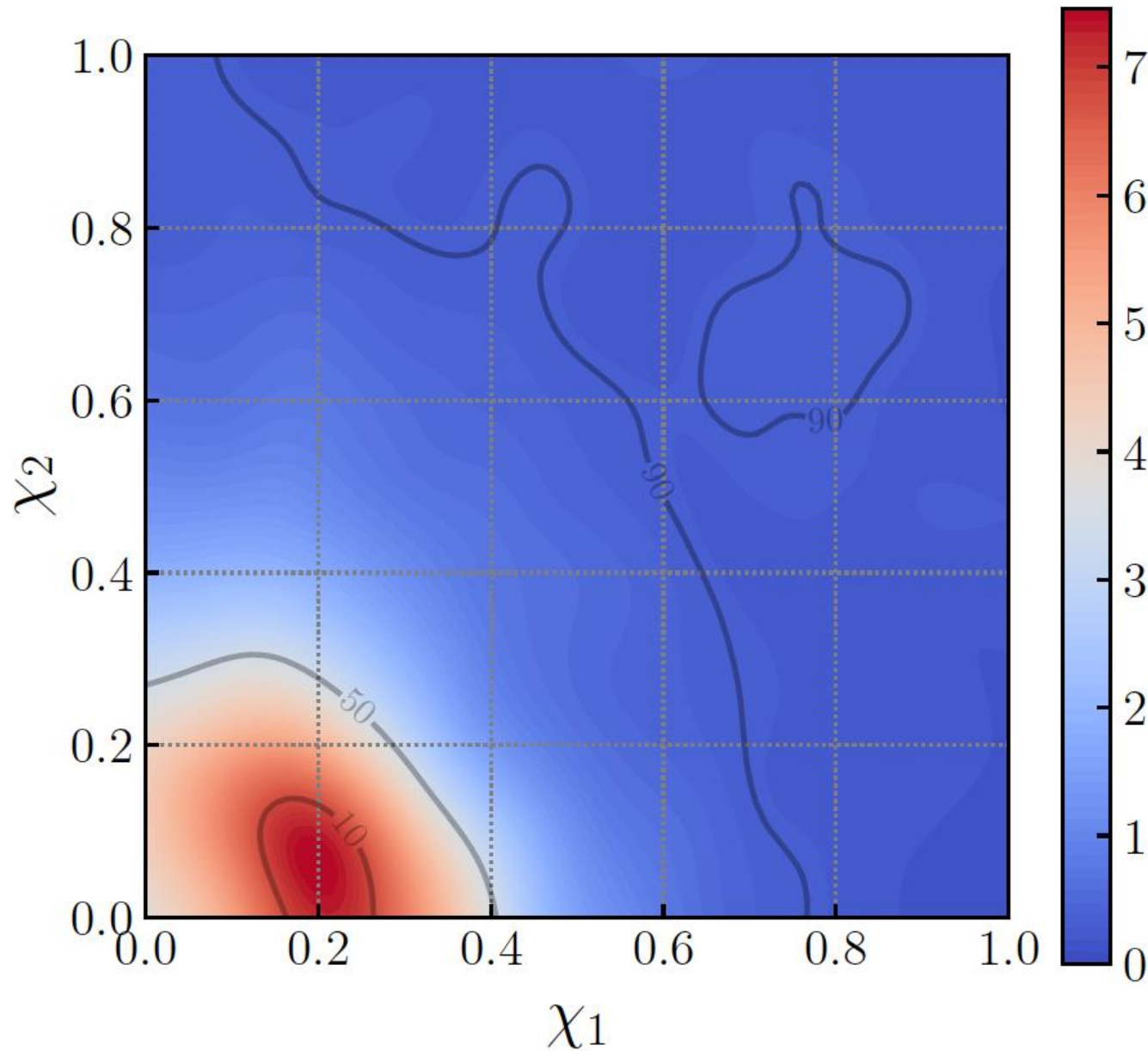
Effective and Final Spin

JGB, Nuño-Siles, Ruiz Morales [2010.13811].

Isotropic and Spin=0

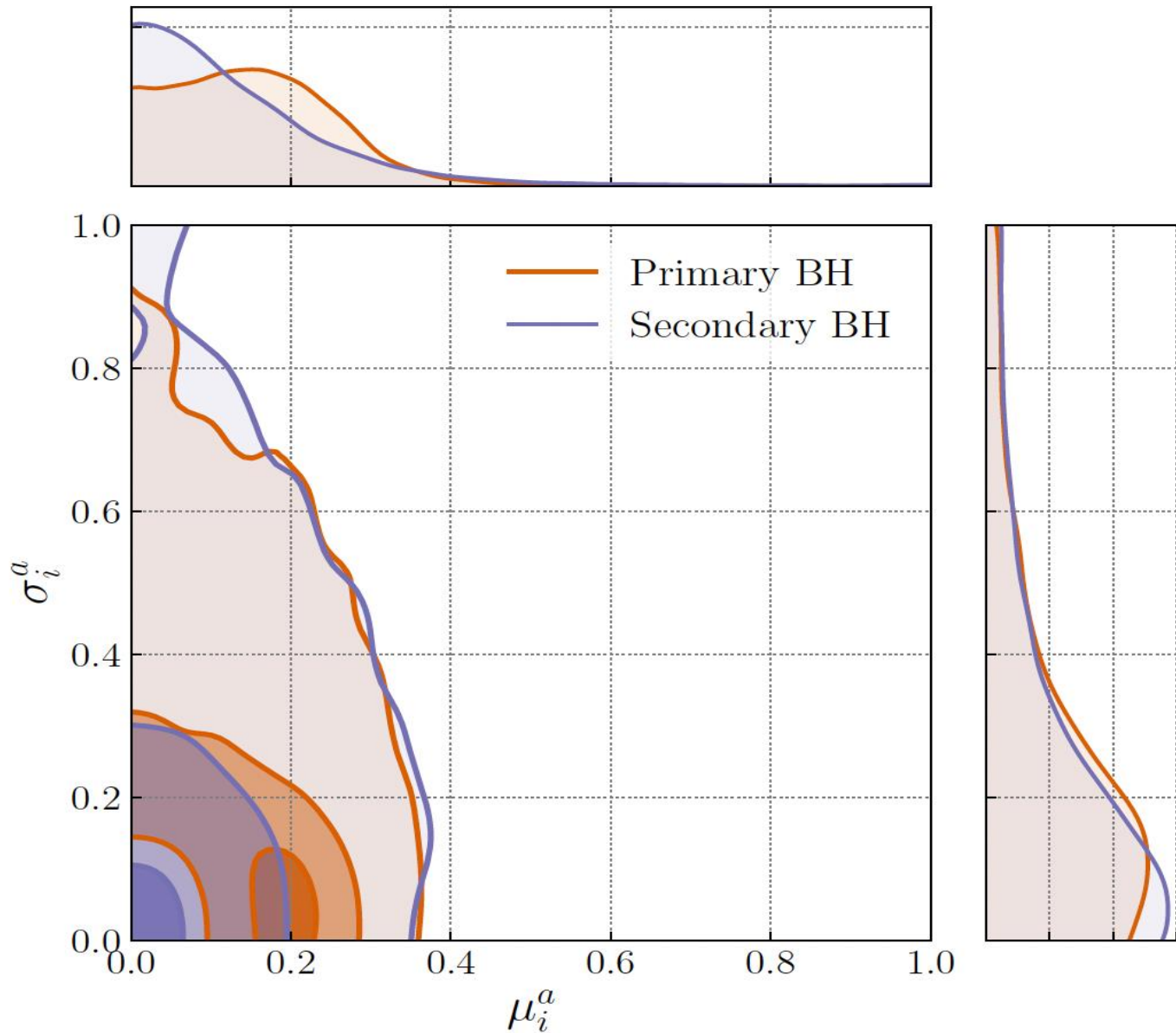


Spin distributions GWTC-3



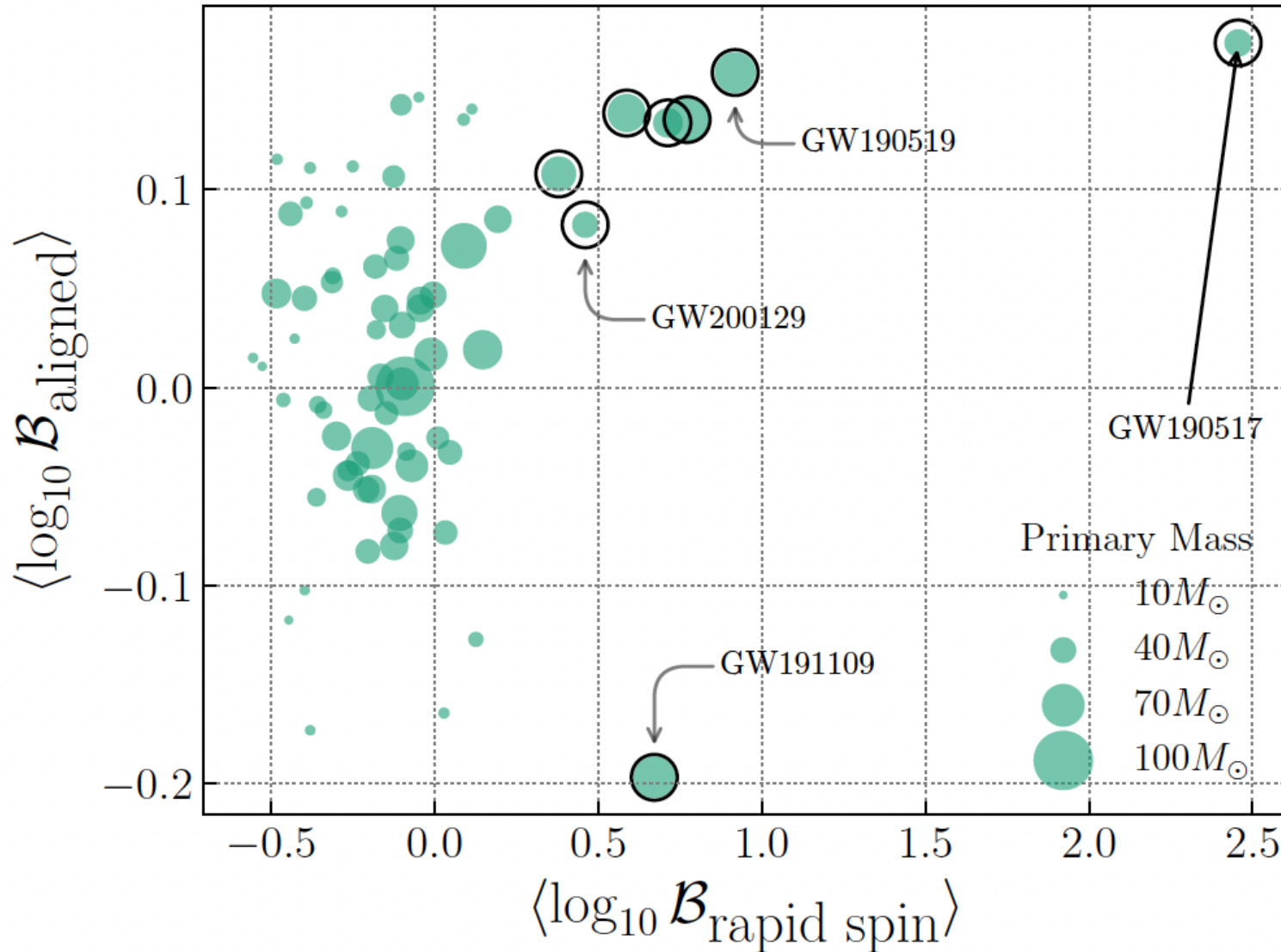
Hussain et al. [2411.02252]

Spin distributions GWTC-3



Hussain et al. [2411.02252]

Spin distributions GWTC-3

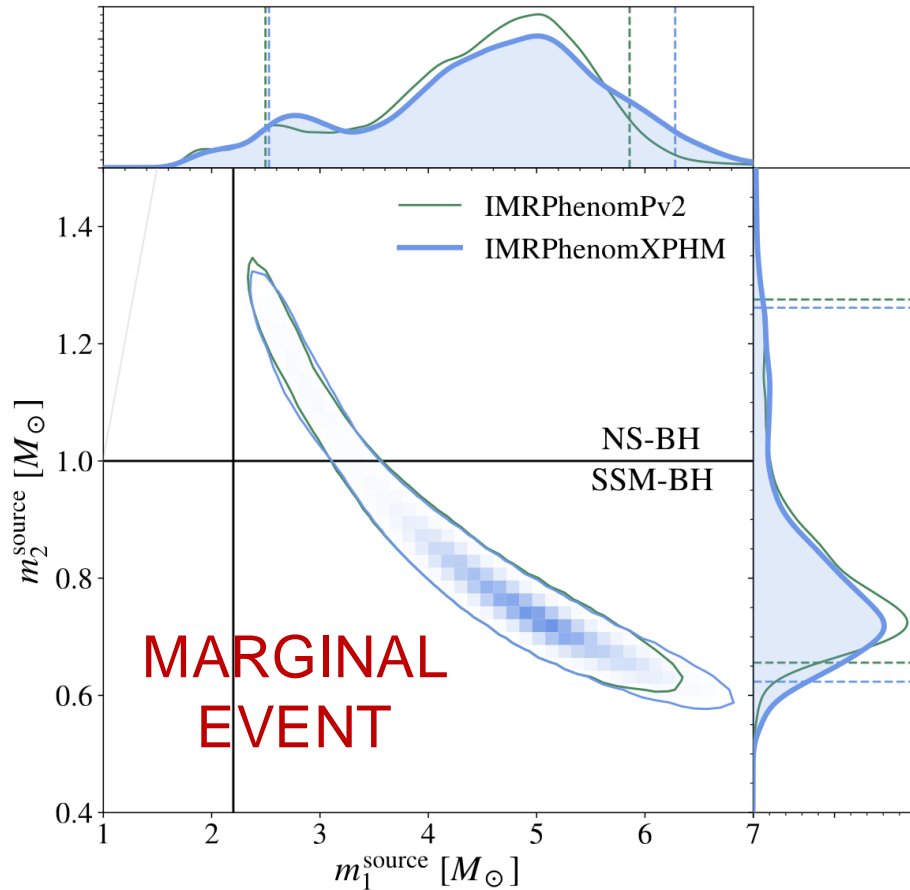


Hussain et al. [2411.02252]

Are there PBH in LIGO/Virgo?

SSM170401

Morras et al. [2301.11619]

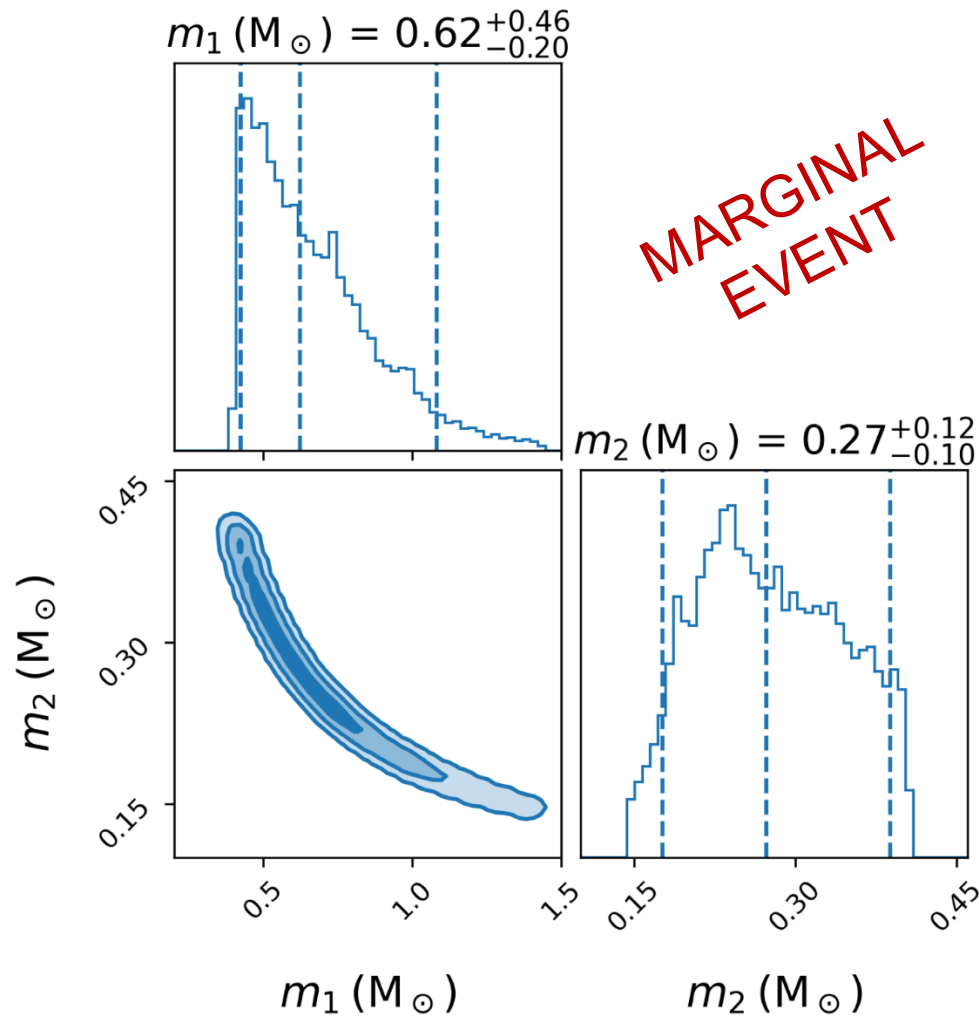


Parameter	IMRPhenomPv2	IMRPhenomXPHM
Signal to Noise Ratio	$7.98^{+0.62}_{-1.03}$	$7.94^{+0.70}_{-1.05}$
Primary mass (M_\odot)	$4.65^{+1.21}_{-2.15}$	$4.71^{+1.57}_{-2.18}$
Secondary mass (M_\odot)	$0.77^{+0.50}_{-0.12}$	$0.76^{+0.50}_{-0.14}$
Primary spin magnitude	$0.32^{+0.47}_{-0.26}$	$0.36^{+0.46}_{-0.30}$
Secondary spin magnitude	$0.48^{+0.46}_{-0.43}$	$0.47^{+0.46}_{-0.42}$
Total mass (M_\odot)	$5.42^{+1.10}_{-1.65}$	$5.47^{+1.43}_{-1.68}$
Mass ratio ($m_2/m_1 \leq 1$)	$0.17^{+0.34}_{-0.05}$	$0.16^{+0.34}_{-0.06}$
χ_{eff} [51, 52]	$-0.06^{+0.17}_{-0.32}$	$-0.05^{+0.22}_{-0.35}$
χ_p [53]	$0.28^{+0.34}_{-0.21}$	$0.33^{+0.33}_{-0.26}$
Luminosity Distance (Mpc)	119^{+82}_{-48}	124^{+82}_{-48}
Redshift	$0.028^{+0.018}_{-0.010}$	$0.028^{+0.017}_{-0.011}$
Ra ($^\circ$)	-2^{+34}_{-35}	-1^{+34}_{-37}
Dec ($^\circ$)	47^{+14}_{-26}	46^{+14}_{-29}
Final mass (M_\odot)	$5.34^{+1.11}_{-1.70}$	$5.40^{+1.45}_{-1.73}$
Final spin	$0.39^{+0.24}_{-0.07}$	$0.42^{+0.22}_{-0.10}$
$P(m_2 < 1 M_\odot)$	85%	84%

Are there PBH in LIGO/Virgo?

SSM200308

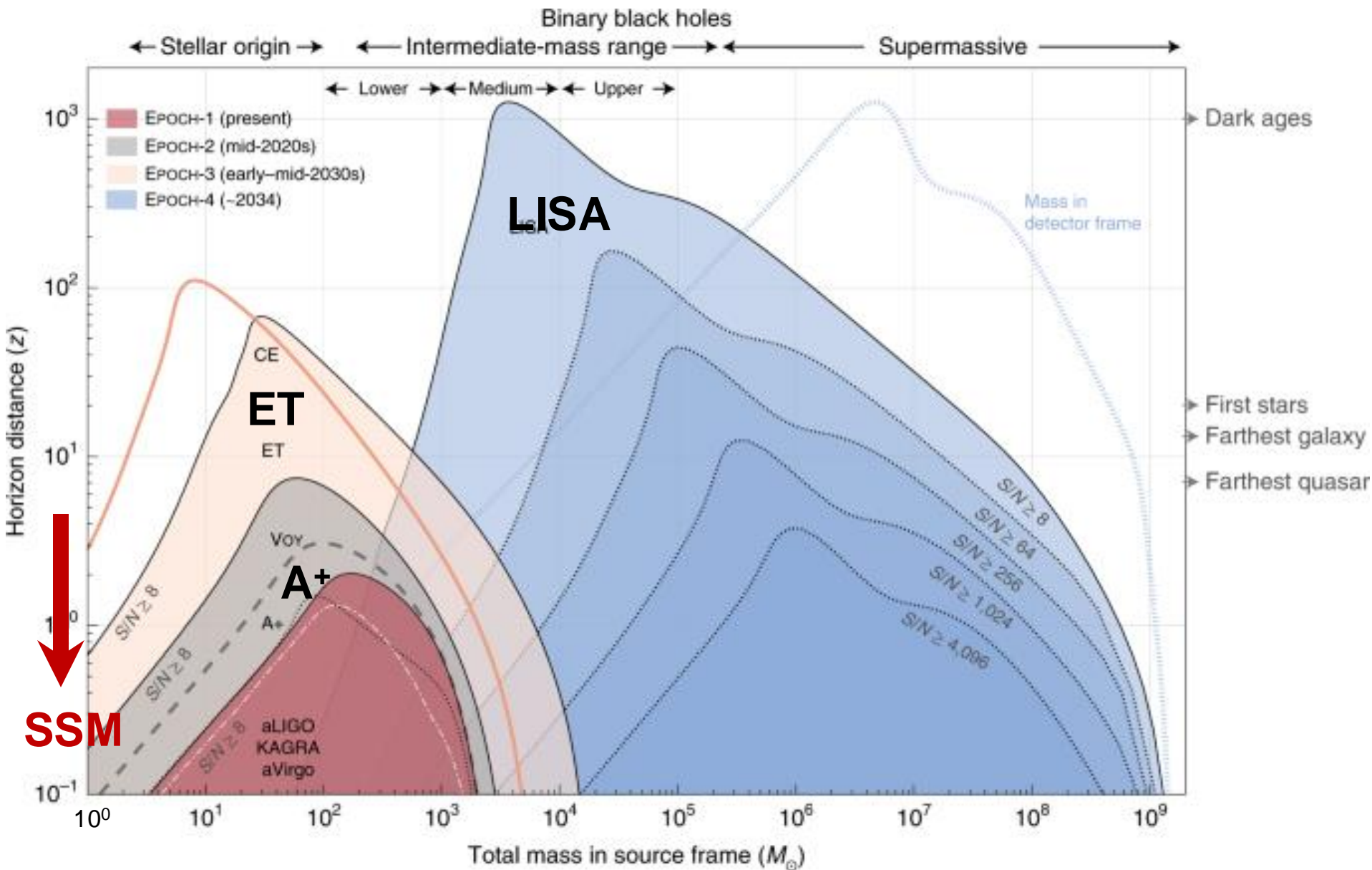
Prunier et al. [2311.16085]



Parameter

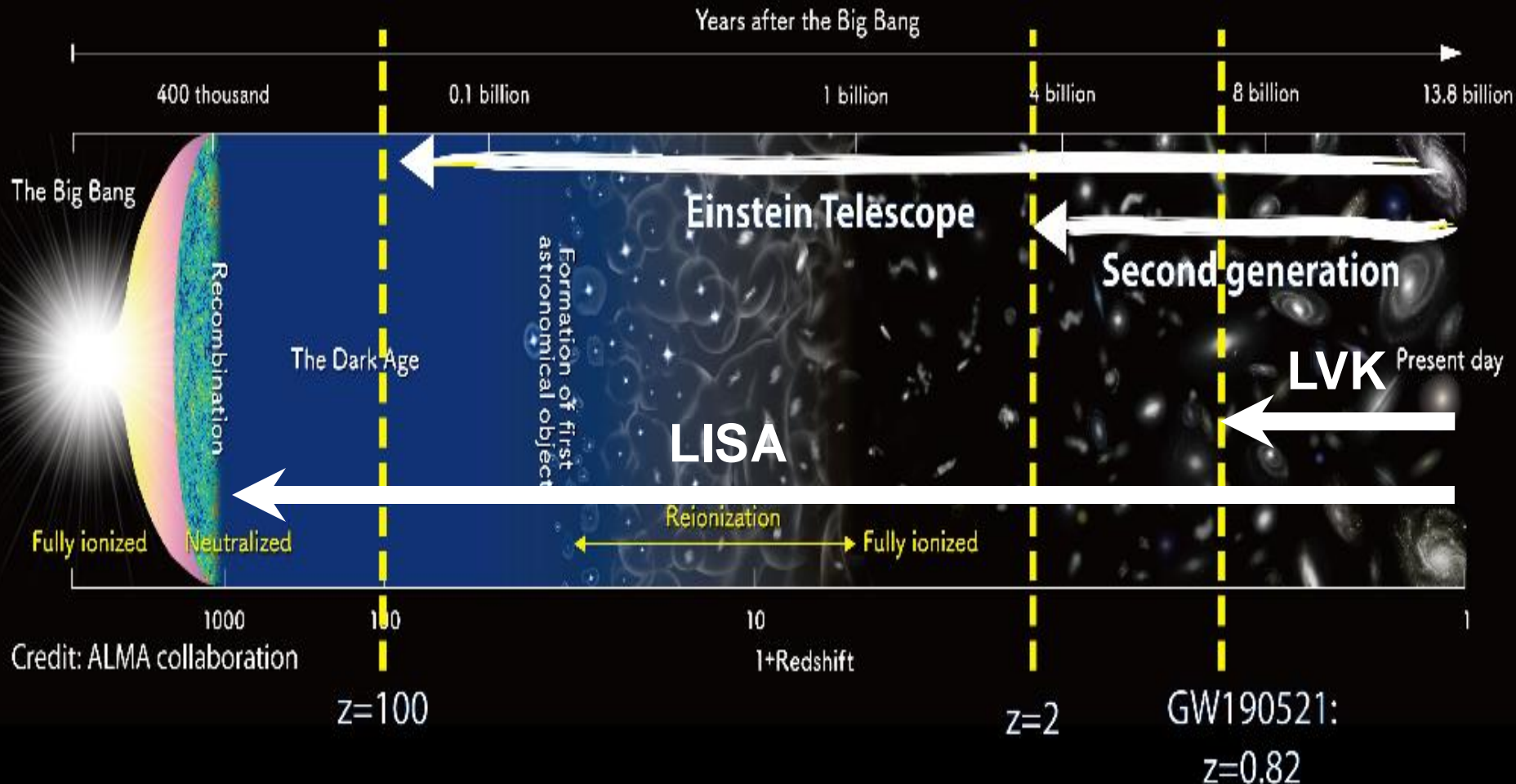
Matched Filter SNR	$8.02^{+0.49}_{-0.85}$
Primary mass (M_\odot)	$0.62^{+0.46}_{-0.20}$
Secondary mass (M_\odot)	$0.27^{+0.12}_{-0.10}$
Primary spin magnitude	$0.66^{+0.13}_{-0.25}$
Secondary spin magnitude	$0.44^{+0.33}_{-0.39}$
Total mass (M_\odot)	$0.88^{+0.35}_{-0.08}$
Detector-frame chirp mass (M_\odot)	$0.3527^{+0.0003}_{-0.0001}$
Mass ratio ($m_2/m_1 \leq 1$)	$0.44^{+0.48}_{-0.28}$
χ_{eff} [27, 28]	$0.41^{+0.08}_{-0.04}$
χ_p [29]	$0.37^{+0.24}_{-0.24}$
Luminosity Distance (Mpc)	90^{+43}_{-39}
Redshift	$0.02^{+0.01}_{-0.01}$
$P(m_1 < 1 M_\odot)$	92%
$P(m_2 < 1 M_\odot)$	100%

BBH sensitivity in future G3 GW



The future of GW (G3)

Detection horizon for black-hole binaries



Conclusions

- Quantum diffusion inevitably generates PBH
- Thermal history predicts PBH with multimodal mass distribution $\sim 10^{-5}, 1, 100, 10^5 M_{\odot}$ ($10^{-10} M_{\odot}$ also?)
- The predicted PBH spin and mass distribution has been measured by LIGO/Virgo + OGLE/Gaia around 1-100 M_{\odot} (features: peak & plateau)
- Other peaks could be explored with microlensing
- PBH scenario can explain various cosmic conundra
- Paradigm shift in Structure Formation of the Universe
- Very rich phenomenology: multiscale, multiepoch, multiprobe \Rightarrow Future GB detectors (ET, CE, LISA)